JOURNAL OF MATERIALS SCIENCE 24 (1989) 4177–4208

Review
Methods for improving the mechanical properties of oxide glasses

I. W. DONALD
Atomic Weapons Establishment, Aldermaston, Berkshire, UK

Methods are reviewed for improving the mechanical properties of oxide glasses. These are divided into surface and bulk techniques and include thermal and chemical strengthening, controlled crystallization, and particle, fibre and whisker reinforcement. The merits and limitations of individual techniques are compared and discussed. In conclusion, a number of applications for these materials are briefly outlined.

1. Introduction

Man-made oxide-based glasses, initially in the form of decorative glazes, appeared around 6000 years ago in Mesopotamia and Egypt. Around the beginning of the first century AD, the developing art of glass-making spread throughout the countries of the Roman Empire. In the seventeenth century, man's perception of the universe was transformed by the advent of the optical telescope. At the present time, glasses are used in diverse and far-ranging applications, including the architectural, transportation, engineering, electronic, telecommunications and aerospace industries. Glasses in the form of optical fibres are today in the process of revolutionizing the telecommunications and electronic fields, and glasses are recognized as one of the most useful and important classes of material known. For many applications, however, the intrinsic brittle behaviour of glasses, with their high susceptibility to catastrophic and often impressive failure, is a serious disadvantage. Over the years, therefore, many attempts have been made at improving the mechanical properties of these materials, either by making them less prone to failure at low applied stresses, or by preventing the catastrophic disintegration of materials during failure.

Some of the methods that have been used for improving the mechanical properties of glasses are considered in this review, and their individual merits and limitations are discussed. Methods are classified under two broad headings, namely surface or bulk techniques. Surface methods are used generally for increasing the strength of glass or improving its susceptibility to the influence of surface defects, whilst bulk methods have been employed successfully for increasing both the strength and fracture toughness of these materials. Many of the methods to be described, for example particle and fibre reinforcement, can also be applied to other ceramic materials in addition to oxide glasses; however, emphasis is given throughout this review only to glassy oxide materials. In conclusion, a number of applications and potential applications for strengthened and toughened glasses are outlined.

2. Mechanical properties of glasses

The mechanical properties of oxide glasses, in which covalent–ionic bonding predominates, are dominated by brittle behaviour. For all practical purposes, these materials exhibit completely elastic behaviour up to their breaking points, with no indication of significant macroscopic ductility, at least at temperatures less than the glass transition temperature, T_g, and at ambient hydrostatic pressures. The theoretical strength of glass has been estimated to be of the order of $E/10$, where E is Young's modulus [1]. This suggests that oxide glasses should exhibit strengths of the order of ≈ 7000 MPa. In practice, however, useful strengths rarely exceed 100 MPa. This large discrepancy between theoretical and practical strengths has been explained on the basis of defects in glass, particularly defects at the surface, which act as stress concentration sites, enabling the theoretical strength limit to be exceeded locally for very small applied stresses. Griffith [2, 3], based on earlier work by Inglis [4] and Kolosoff [5] emphasized this weakening influence of defects on existing materials, although the significance of his early work went largely unappreciated for many years [6].

It had been shown by Inglis [4] for example, that the maximum stress at a crack tip, σ_m, could be given by

$$\sigma_m = 2\sigma\,(c/\varrho)^{1/2} \qquad (1)$$

where σ is the applied stress, c the crack length, and ϱ the radius of curvature of the crack tip.

Griffith followed on from this work by developing a theory, based on energy considerations, for the propagation of pre-existing cracks, in which he showed, for conditions of plane stress, that the fracture stress, σ_f, of a brittle material, could be given by the relationship

$$\sigma_f = (2E\gamma/\pi c)^{1/2} \qquad (2)$$

where γ is the fracture surface energy.

0022-2461/89 $03.00 + .12

For conditions of plane strain, the relationship becomes

$$\sigma_f = [2E\gamma/\pi(1 - \nu^2)c]^{1/2} \qquad (3)$$

where, ν is Poisson's ratio.

It follows from these expressions (Equations 1 to 3) that sharp cracks act as mechanical levers by concentrating the stress at the crack tip. The smaller the value of ϱ, or the higher the value of c, the greater this stress concentration effect will be and, consequently, the lower the strength of the material. The low strengths of oxide glasses and related materials are thereby a direct consequence of the presence of stress concentrating defects, and this is coupled, for these brittle materials, with a lack of significant operative stress relieving mechanisms. Cracks once initiated will, therefore, propagate unimpeded, under the influence of a critical applied load, and hence failure is catastrophic. This is in contrast to ductile metals where dislocation motion can relieve stresses at crack tips, effectively blunting the cracks and therefore making these materials less susceptible to catastrophic failure.

Extension of Griffith's earlier work has led to the field of fracture mechanics and the concept of a critical stress intensity factor, K_c, (K_{Ic} for conditions of plane strain), which is directly related to the stress at which a crack can propagate continuously, i.e., catastrophically. The critical stress intensity factor is a measure of the "toughness" of a material, or its resistance to crack propagation and, unlike strength, it is usually regarded as a materials constant. The strength of a brittle material is given by

$$\sigma_f = K_{Ic}/Yc^{1/2} \qquad (4)$$

where Y is a dimensionless constant which takes into account sample geometry and loading characteristics. The strength is, therefore, dependent on the intrinsic fracture toughness of the material and the severity of defects. Specific details of fracture mechanics analyses and experimental techniques, with particular attention to ceramic materials, are described more comprehensively elsewhere (e.g. [7]).

Another parameter used frequently to measure the toughness of a material is the work of fracture [8]. This is defined as the work done per unit area in propagating a crack. This technique measures the mean fracture energy for the total process, unlike the fracture mechanics treatment which gives information on the fracture initiation energy. In general, the crack initiation energy is not equal to the energy required to propagate a crack, but may be greater in the case of a brittle material, or less in the case of a ductile or fibre-reinforced material. It should be noted, however, that unlike fracture toughness, K_{Ic}, work of fracture has been found to be strongly dependent on loading geometry (e.g. [9]) and therefore, like mechanical strength, it is not a materials constant.

In addition to low mechanical strength and fracture toughness, oxide glasses suffer from another serious disadvantage that further limits their usefulness, particularly as structural load-bearing materials. This is the phenomenon of static fatigue whereby, depending on the environment, small, pre-existing cracks or defects grow under the influence of an applied stress which is considerably lower than the normal fracture stress of the material. When a critical flaw size is reached under these conditions, flaw propagation becomes catastrophic. The overall mechanical behaviour of glass, therefore, depends strongly on the environment, and is also a function of time. Static fatigue data for oxide glasses have been reviewed in detail by Adams and McMillan [10]. Static fatigue can be likened to stress corrosion of crystalline metallic materials where existing surface defects grow under the influence of an external stress which is below the normal failure stress of the material. For oxide glasses, the corrosive medium is usually water, which is normally present in the environment, although other agents can invoke similar, but generally lesser, effects [11].

Some typical mechanical property data comparing glasses and other materials are given in Table I.

3. Methods for improving the mechanical properties of glasses

There are a number of methods by which the mechanical properties of oxide glasses can be improved, as summarized in Table II. Many of these methods can lead to very substantial increases in fracture strength of glasses, although toughness, and in particular resistance to catastrophic failure, may not be improved upon significantly. Other methods can lead to improvements in toughness at the expense of strength, whilst others are effective at improving strength and toughness simultaneously. Methods can be very broadly classified into surface or bulk techniques. Many of the techniques to be described, particularly surface compressive methods, are also quite effective at limiting the deleterious effects of static fatigue.

3.1. Surface methods for improvement in strength

Fracture of a brittle solid is almost invariably initiated from the surface due, as already described, to the presence of stress intensifying defects; thus, it is feasible to increase the strength of these materials by removing or minimizing such defects, or by placing the surface in a state of compression. Methods for accomplishing this are outlined below.

3.1.1. Etching and related techniques

Surface damage can be removed very successfully by, for example, etching using a dilute aqueous solution of HF (or, ideally, a mixture of HF and another acid, e.g. H_2SO_4 or HCl, that will dissolve water-insoluble fluoride compounds formed by reaction between HF and the glass). Bulk glasses exhibiting very high mechanical strengths, in excess of 1000 MPa, have been produced by this method [12–14], in which cracks are either removed almost completely or crack tip radii increased significantly [15]. Reaction with other liquid reagents, even water [16], can lead to strength enhancement, and etching with anhydrous molten salts, for example $NaBF_4$ in $NaNO_3$ or KBF_4 in KNO_3 [17], can enhance strength. Similarly, the related

TABLE I Some typical values for the mechanical properties of various materials (in dense bulk form)

Material	Maximum flexural strength (MPa)	Work of fracture ($kJ\,m^{-2}$)	Fracture toughness, K_{Ic} ($MPa\,m^{1/2}$)	E (GPa)	Hardness (VPN)
Epoxy resin	100	0.2	0.8	2–4	–
Fused silica	50	0.002	0.6	75	640
Oxide glass	100	0.003	0.6	140	700
Glass–ceramic	400	0.005	0.8–2.6	150	950
Thermally strengthened glass	500	–	–	140	700
Chemically strengthened glass	900	–	–	140	> 700
Chemically strengthened glass-ceramic	1500	–	–	150	950
MgO	140	0.3	< 3.0	250	690
Alumina	500	0.05	< 4	400	1400–1900
Si_3N_4	800	< 0.17	< 7	320	1600–1800
SiC	> 400	< 0.05	< 5	440	2400–2800
B_4C	400	–	< 5	450	2800–3200
Diamond	–	0.01	3.4	960	≈ 8000
Y_2O_3 partially stabilized zirconia	650	–	6.4	200	1300
16 vol % ZrO_2 dispersion-strengthened alumina	1200	–	15.0	–	–
Cast iron*	320	4	≈ 10	–	–
Aluminium alloy*	580	> 7	20–100	80	140
Ductile high strength steel*	1800	5–130	30–250	–	200–550
High strength superalloy*	1400	–	–	200	200–450
High strength titanium alloy*	1420	–	55	125	–

*Tensile data

technique of "flame polishing" in which the surface of glass is softened by heating, leading to removal or healing of flaws, is a standard method for improving the mechanical properties of glass articles. Simple annealing can also increase the strength of glass by blunting crack tips [18], although heating at temperatures less than the glass transition temperature can have the reverse effect and lead to a decrease in strength [19]. Unfortunately, the increases in strength effected by these processes are very transient in nature, and normal handling rapidly reduces the strength of glass articles to values approaching their former low values. After etching or subjecting to other surface treatments, however, the surface may be protected to some degree by application of a suitable protective coating; this will be described in more detail later.

3.1.2. Formation of a surface compressive layer

A number of methods have been devised for generating surface compressive stresses. Strength increases are achieved because the compressive stress at the surface must be overcome before defects are subjected to tensile forces. As a very rough guide, the strength of a glass article with a surface compressive stress is equal to the magnitude of the compressive stress plus the normal fracture strength of the untreated material. In order to impart useful strength the depth of a compressive layer must generally be greater than the size of typical flaws, i.e. greater than 50 μm.

3.1.2.1. Thermal treatments. One method by which a state of surface compression can be achieved is to cool the glass rapidly from a temperature above the glass transition temperature. Rapid cooling, in this sense, normally involves quenching by air jets or, more recently, by jets of liquid, or even gas fluidized particulate matter [20], directed at the glass surface. This process gives rise to the familiar "toughened", or "tempered" glass, used for many years in the automobile industry. In this respect, the common phrases employed, that is to say, "toughened" or "tempered", can be misleading since it is the strength of the glass and its strain to failure that are increased, and strictly speaking toughness is only increased very marginally; and when fracture does occur, it is still catastrophic. The surface of the glass cools more rapidly than the interior under the quenching conditions; thus, the temperature of the surface rapidly falls below T_g, the surface then behaving as a rigid, elastic Hookean solid. Visco-elastic deformation of the interior of the glass is still possible, however, during the stage when the glass surface becomes rigid and contracts. Stresses in the interior are therefore relaxed initially until a stage is reached when the interior also becomes rigid. As, at this stage, the temperature of the interior is still higher than that of the surface, contraction of the interior is opposed by the surface; consequently the surface is placed in a state of compression as the temperature differential equilibrates. A balancing tensile stress is developed in the interior of the glass. The stress distribution obtained by this method is

TABLE II Summary of methods for improving the mechanical properties of glasses

Method	Applicable to	Comments/Mechanism
Surface modification		
(a) Etching and related techniques	most glasses	removal of surface damage
(b) Thermal strengthening	limited to glasses of $t \geqslant 2\,\text{mm}$, and $\alpha \geqslant 4.5 \times 10^{-6}\,{}^{\circ}\text{C}^{-1}$	surface "solidifies" before interior: this gives surface compression
(c) Chemical strengthening	many alkali-containing glasses, particularly alkali alumino-silicates	exchange of small ions in glass surface by larger ions to give higher density surface: this gives surface compression
(d) Surface crystallization	limited to a number of specific compositions	formation of lower expansion surface crystallized layer: this gives surface compression
(e) Thin coating	most glasses	protection of pristine surface
(f) Cladding	glasses of $\alpha >$ cladding	coating of surface with compatible lower expansion material: this gives surface compression
Bulk methods		
(a) Bulk crystallization	many silicate glasses	internal nucleation and growth of crystals to give fine-grained, porosity-free polycrystalline glass–ceramic material: grain boundaries impede crack propagation
(b) Particle reinforcement	many glasses	dispersion-strengthened or age-hardened systems: this gives limited load transfer and particle deformation; particles can impede crack propagation
(c) Transformation toughening	glasses containing ZrO_2	special case of dispersion-strengthening involves stress-induced structural transformation in particulate phase during crack propagation
(d) Fibre reinforcement	most glasses	crack impedement, load transfer, fibre deformation/pull-out, matrix microcracking
(e) Whisker reinforcement	most glasses	crack impedement, load transfer, whisker pull-out for large aspect ratios, matrix microcracking
(f) Laminated structures	many glasses	alternate layers of glass and thermoplastic material to give composite sandwich

approximately parabolic, as illustrated in Fig. 1. As a rough guide, the compressive stress at the surface, σ_c, is approximately twice the value of the tensile stress, σ_t, in the interior, and the thickness of the compressive layer, t_c, is around 20 to 25% that of the glass itself.

The magnitude of the surface compressive stress attainable by thermal methods is limited by a number of factors. These include limitations imposed by the maximum practical cooling rate achievable and the thermal characteristics of the glass, in addition

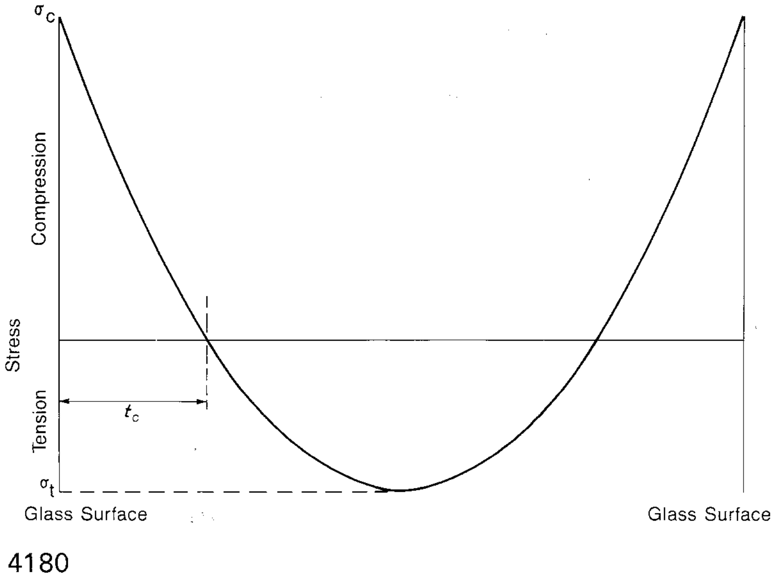

Figure 1 Typical stress profile of a thermally strengthened glass.

to geometrical considerations. These tend to limit thermal methods to glass articles of relatively simple shape, moderately high thermal expansion, and thicknesses greater than about 1.5 to 2 mm. The maximum strength realized in practice is of the order of 350 to 400 MPa, which is approximately three to five times stronger than the untreated glass.

As a consequence of the high strengthening stresses, a significant amount of strain energy can be stored in a thermally strengthened glass. When fracture occurs, by penetration of a crack through the compressive zone into the tensile region, this strain energy is released and appears largely in the form of the surface energy of the fragments produced. Consequently, depending on the precise magnitude of the internal tension, a large surface area may be created, and this can give rise to a considerable number of small, approximately equi-sized glass fragments. Because the interior of the glass is in a state of tension, it is important that the parent glass is of very high quality. If, for example, internal defects are present, they may lead to premature failure of the article, either during the quenching process or, more deleteriously, at a later date whilst the article is in service.

Thermal methods were first employed in an attempt to improve the strength of glass articles in the 1870s, but it was not until the 1920s that practical methods of achieving the cooling rates required, without damaging the glass, were devised, as reviewed recently by Gardon [21]. Further more detailed information on thermal strengthening, including a comprehensive description of the theoretical concepts, is also provided by Gardon.

3.1.2.2. Surface crystallization. A number of reports have been given of glasses strengthened by a simple heat treatment in air to give a surface crystallized layer which has a lower thermal expansion than that of the bulk glass. On cooling these materials from the crystallization temperature, the interior attempts to contract more than the surface, and so places the surface in compression. As for the thermally strengthened glasses, a balancing tensile stress is created in the interior. Unlike the parabolic stress distribution noted for thermally strengthened glasses, however, the stress distribution obtained by surface crystallization is usually very different in character. In particular, the transition from compression to tension may be very sharp. This sharp transition can lead to degradation of the glass article due to spalling of the surface layers, either during the surface crystallization process, or later due to the influence of static fatigue.

Glasses most suitable for strengthening by surface crystallization include lithium alumino-silicates, where a crystalline surface layer of low expansion β-spodumene or β-eucryptite can be produced, as reported by Stookey *et al.* [22], Petticrew *et al.* [23], and Keifer *et al.* [24], and lithium silicates, as noted by McMillan *et al.* [25]. Other compositions include zinc alumino-silicates, where low expansion willemite or stuffed keatite can be formed, as reported by McMillan *et al.* [26], and McMillan and Partridge [27–29].

Strengthening has also been noted by Adams and McMillan [30] for calcium aluminate based glasses, surface crystallized to produce a crystalline phase with a similar thermal expansion to that of the bulk glass. In this instance, however, the strength increases involved were generally less than that obtained by formation of a lower expansion surface, and strengthening was attributed to the limiting in size of Griffith-type flaws in the glass surface. Attempts have been made at surface crystallizing other glass compositions, but with only limited success, as reviewed recently by Partridge [31].

In order to promote surface crystallization, rather than crystallization of the bulk material, it is necessary to provide crystal nucleation sites on the glass surface. This has been accomplished by various techniques aimed at providing, for example, an even distribution of very fine scratches in the surface from which crystals can nucleate and grow [25–27]. One of the most successful methods has been polishing, followed by vibration in a bed of sand or silicon carbide grit using a vibratory table [25]. On subsequent heat treatment of the glass, this provides a homogeneous distribution of small evenly spaced crystals at the surface.

Some representative mechanical property data for surface crystallized glasses are given in Table III.

3.1.2.3 Chemical treatments. In addition to the thermal treatments which yield surface compressive stresses, chemical methods are also feasible. Chemical methods have the distinct advantage that almost any geometry can be employed and, in addition, very thin sections less than 2 mm in thickness can be used, because the method does not rely on the setting up of thermal gradients. Furthermore, in contrast to thermal strengthening, glasses with low or even zero thermal expansion coefficients can be treated successfully by chemical methods. Treatment is also carried out at temperatures lower than T_g so that problems associated with viscous deformation and consequent permanent distortion of the body, which can occur during thermal treatments, are alleviated.

Chemical strengthening generally relies on exchanging small ions in a glass surface by larger ions. The larger ions can be provided by treating the glass article in a molten salt bath. Substitution of larger for smaller ions in the glass surface tends to expand the glass structure, but this expansion is restricted by the glass interior. Consequently, the surface of the glass is placed in a state of compression, and a balancing tensile stress is again generated in the interior. The stress profile of chemically strengthened glasses is similar to that of a surface crystallized glass, although the stress gradients are not normally as steep, and the transition from compression to tension is less severe; a typical stress profile for a chemically strengthened glass is illustrated in Fig. 2.

The successful use of chemical ion-exchange strengthening was first reported by Kistler in 1962 [32] for soda-lime-silica glasses treated in potassium nitrate. The driving force for chemical ion-exchange is the chemical concentration gradient, and this depends on the diffusivity of the respective ions.The highest

TABLE III Details of surface crystallized glasses

Glass number*	Heat-treatment conditions		Major crystalline phase formed	Thickness of surface layer (μm)	Flexural strength		Reference
	Temperature (°C)	Time (h)			Before (MPa)	After (MPa)	
(a) *Lithium alumino-silicate glasses*							
1	890	18	β-eucryptite	80	–	600–700	[22]
1	860	48	β-eucryptite	80	–	600–700	[22]
1	890	20	β-eucryptite	100	–	600–700	[22]
1	860	60	β-eucryptite	100	–	600–700	[22]
(b) *Zinc alumino-silicate glasses*							
2	800	2	willemite	–	–	366	[27]
	+850	+2					
3	800	2	willemite	–	–	372	[27]
	+850	+2					
4	800	2	willemite	–	–	439	[27]
	+850	+2					
5	800	2	willemite	–	–	414–517	[27]
	+850	+2					
6	800	2	willemite	–	–	524	[27]
	+850	+2					
7	800	2	willemite	–	–	607–634	[27]
	+850	+2					
8	800	2	willemite	–	-	708	[27]
	+850	+2					
9	750	0.5	–	–	–	493	[28]
10	750	0.5	–	–	–	551	[28]
11	750	0.5	–	–	–	584	[28]
12	750	50	albite	60	70	300	[29]
12	800	16.7	albite	60	70	300	[29]
13	800	9.4	stuffed keatite	90	70	620	[29]
13	850	1.9	stuffed keatite	90	70	620	[29]
14	700	16.7	stuffed keatite	100	70	670	[29]
14	800	0.5	stuffed keatite	100	70	670	[29]
14	850	0.1	stuffed keatite	100	70	670	[29]
15	800	9.9	stuffed keatite	160	70	830	[29]
15	850	2.4	stuffed keatite	160	70	830	[29]
(c) *Calcium zinc alumino-silicate glasses*							
16	820	1.0	willemite	11	90	145	[30]
16	820	2.5	willemite	40	90	245	[30]
16	820	4.3	willemite	49	90	275	[30]
16	840	1.0	willemite	23	90	180	[30]
16	840	2.5	willemite	54	90	283	[30]
(d) *Calcium aluminate glasses*							
17	850	3	–	20	120	510	[30]

*Specific glass compositions are given in Table VI

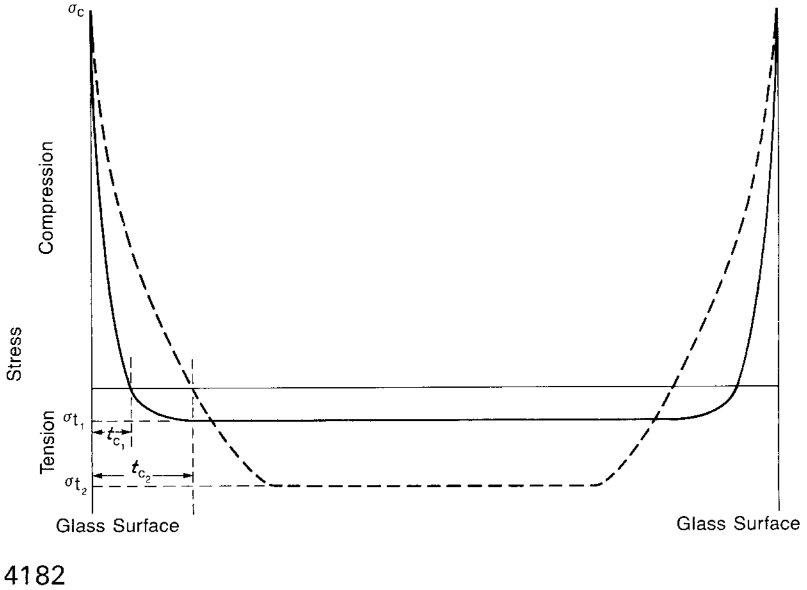

Figure 2 Typical stress profile of a chemically strengthened glass.

TABLE IV Summary of ion-exchange treatments, ionic radii differences and maximum compressive stresses

Basic glass composition	Salt bath	Mechanism	Ionic radius difference (nm)	Approximate volume change* ($\mu m^3 g^{-1}$)	Maximum induced compressive stress* (MPa)
Li_2O-(Al_2O_3)-SiO_2	$NaNO_3$	$Na^+ \rightleftharpoons Li^+$	0.020	90	620
Na_2O-(Al_2O_3)-SiO_2	KNO_3	$K^+ \rightleftharpoons Na^+$	0.035	220	1450
Li_2O-(Al_2O_3)-SiO_2	KNO_3	$K^+ \rightleftharpoons Li^+$	0.055	310	2000
Li_2O-(Al_2O_3)-SiO_2	$RbNO_3$	$Rb^+ \rightleftharpoons Li^+$	0.071	440	2210
Li_2O-(Al_2O_3)-SiO_2	$CsNO_3$	$Cs^+ \rightleftharpoons Li^+$	0.087	665	3965
MgO-(Al_2O_3)-SiO_2	Li_2SO_4	$2Li^+ \rightleftharpoons Mg^{2+}$	–	–	–

*taken from [58].

diffusivities are generally found for alumino-silicate compositions, although early work [33, 34] indicated that alkali zirconia-silicate systems also exhibited useful diffusivities. These glasses therefore provide the most useful materials by yielding compressive layers of practical thicknesses in realistic treatment times. Using, for example, a lithium alumino-silicate composition, Li^+ ions near the glass surface are replaced by larger Na^+ ions from a sodium salt bath, for example, sodium nitrate [35–45]. Similarly, for sodium alumino-silicate glasses, Na^+ ions would be replaced by larger K^+ ions from a potassium salt bath, for example, potassium nitrate [46–53]. Numerous other ion-exchange treatments have been investigated, including mixed multi-ion exchanges (e.g. [41]), and exchange of Na^+ or K^+ for Rb^+, Cs^+, Ag^+, Cd^{2+}, Zn^{2+} or Cu^+/Cu^{2+} [43, 46, 54–57]. Assuming no stress relaxation or related effects, very high compressive stresses are theoretically feasible by ion-exchange [58], as noted in Table IV.

Ion-exchange is a diffusion-controlled process, thus it is temperature and time dependent. Consequently, the higher the ion-exchange temperature, the shorter the time required to develop a compressive layer of practical thickness. The upper temperature is limited, however, due to the possibility of stress relaxation. Hence, if ion-exchange is carried out at temperatures approaching or exceeding T_g, the stresses generated by the process are quickly relaxed or eliminated by viscous flow of the glass. For a given glass composition, the strength increase achievable by ion-exchange depends on the treatment conditions, i.e. temperature and time. A maximum in strength is normally observed as a function of time, as illustrated in Fig. 3 for a range of glass compositions and treatment conditions. For a given glass composition, maximum strength is achieved at shorter treatment times as the temperature is increased; however, as shown in Fig. 4, due to the result of stress relaxation effects, the overall strength decreases with increasing treatment temperature. Similarly, as shown in Fig. 5, a strength decrease is noted on heating a chemically strengthened glass in air, the magnitude of the decrease being dependent on the temperature and time (e.g. [48, 52]). This is again due to the effects of stress relaxation and ionic diffusion which lead to a reduction in the surface compressive stress. Ion-exchange times, t, may vary from a few minutes to several hundred hours, depending on the precise glass composition, the temperature of the bath, and the depth and magnitude of compressive layer required; a characteristic $t^{1/2}$ dependence is normally observed. A prerequisite for an ion-exchange medium is, of course, that it does not chemically corrode or otherwise degrade the glass surface at the temperature employed. Materials have also been produced by electric field-assisted ion-exchange in which a d.c. field is used to enhance the ion-exchange process [59–64].

Very high mechanical strengths can be achieved using the chemical ion-exchange method, with some reports of materials exhibiting strengths in flexure in excess of 800 MPa [33, 45, 62, 64]. This is nearly an order of magnitude higher than untreated glass, and is a direct consequence of the need to overcome the very

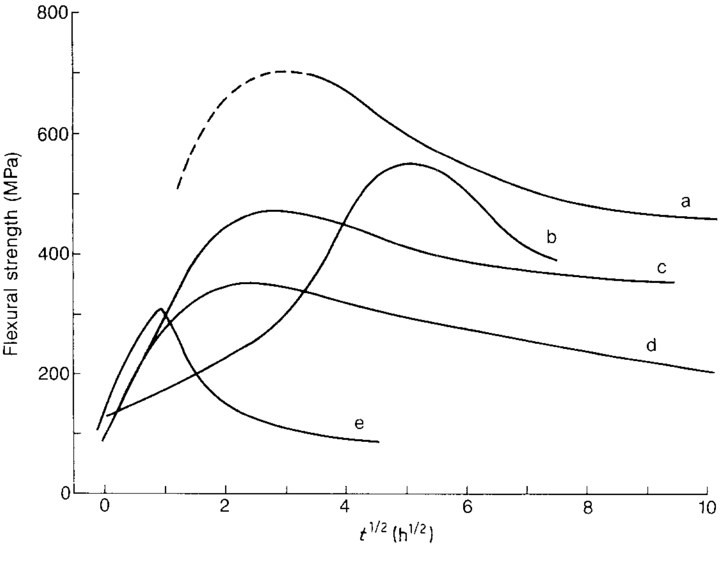

Figure 3 Strength of chemical ion-exchanged glasses as a function of treatment time: a and c lithium magnesium alumino-silicate glasses; after [44] and [45], b sodium silicate glass; after [43], d sodium calcium silicate glass; after [86], e sodium calcium silicate glass; after [47].

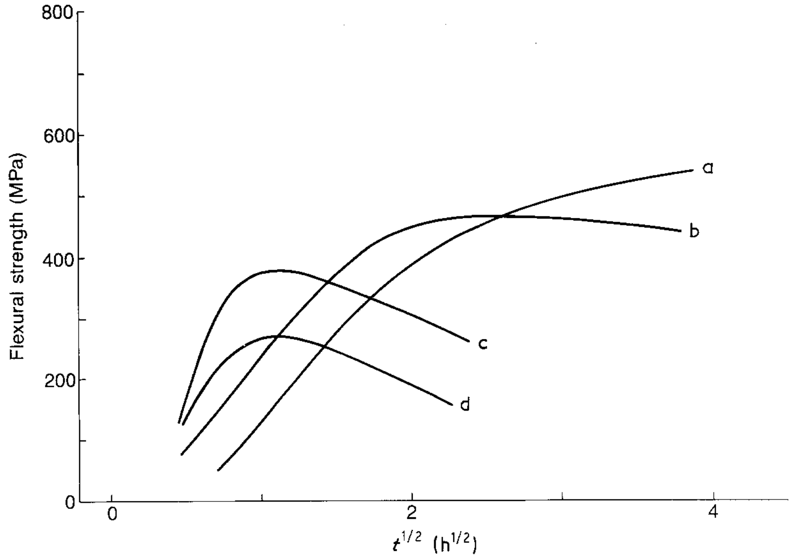

Figure 4 Strength of an ion-exchanged sodium alumino-silicate glass as a function of treatment time at different temperatures (a 450° C, b 500° C, c 550° C, d 575° C) after [34].

high compressive stresses during external loading of the glass, before the strength-impairing effects of surface defects become significant.

The thickness of the compressive layer may vary from a few micrometres to several hundred micrometres, depending on the precise glass composition, treatment conditions and starting glass thickness. In general, the thickness of the layer will be less than that obtained during thermal treatments. If the layer is very thin relative to the overall thickness of the glass (t_{c1} in Fig. 2), the maximum balancing internal tensile stress, σ_{t_1}, may be very small so that, unlike thermally strengthened glasses, these materials can be cut or machined after treatment. On the other hand, for compressive layers that are thick relative to the overall thickness of the glass (t_{c2} in Fig. 2), the internal tensile stress, σ_{t_2}, may be above that required for rapid crack branching, so that when fracture is initiated, by penetration of a crack through the compressive layer, a large number of small, approximately equi-sized glass fragments is produced, almost explosively. This phenomenon has given rise to the special class of chemically strengthened materials, the "frangible" or "command-break" glasses, (e.g. [65]).

In general, the ion-exchanged layer formed during the chemical strengthening of glass articles remains amorphous. A number of reports have shown, however, that treatment in a salt bath at temperatures above the range normally employed can induce crystallization of the ion-exchanged surface layer. This modified technique may be used successfully under certain conditions for increasing the strength very significantly [22, 66, 67]. It is not practised widely, however, due in part to the hazards associated with the use of salt baths at the high temperatures necessary to induce crystallization. In addition, deformation of the article may occur due to viscous flow, since the treatment temperature is greater than T_g.

In addition to glasses, some glass–ceramics have also been treated successfully using chemical ion-exchange [68–70]. These include Na_2O–(K_2O)–Al_2O_3–SiO_2 compositions, nucleated with TiO_2, to give glass–ceramics containing nepheline crystals ($Na_3KAl_4Si_4O_{16}$). Treatment of these glass–ceramics in a potassium salt bath results in the partial or complete exchange of Na^+ ions in the glass–ceramic surface by K^+ ions, resulting in a surface volume increase and the creation of a surface compressive layer. Ultra-high strengths approaching 1500 MPa have been achieved by ion-exchange of these glass–ceramics. Alternatively, treatment of MgO–Al_2O_3–SiO_2 glass–ceramics, nucleated by ZrO_2 or TiO_2 and containing β-quartz crystals, in a lithium

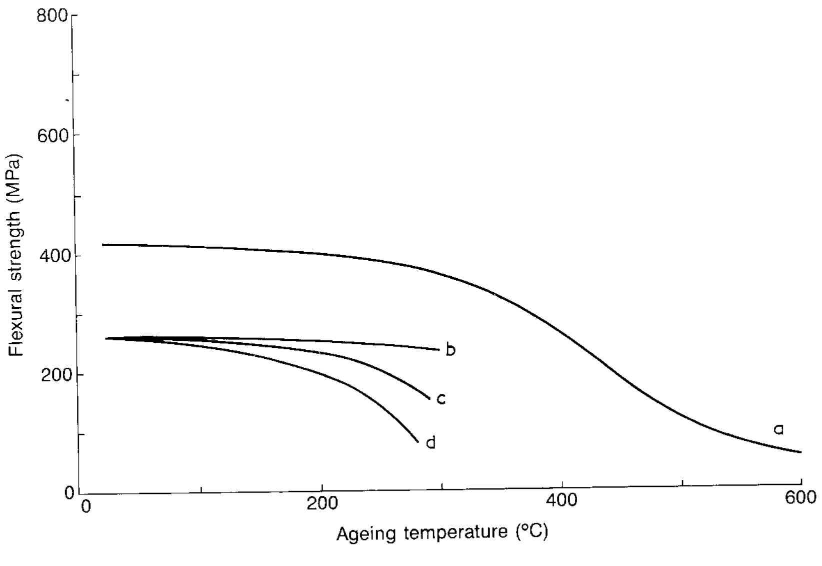

Figure 5 Ambient temperature strength of ion-exchanged glasses as a function of heating temperature in air-glasses aged for times indicated.(a lithium alumino-silicate glass; 4 h, after [48], b unspecified glass; $\frac{1}{4}$ h, c unspecified glass 100 h, d unspecified glass 500 h, after [52]).

TABLE V Details of chemically strengthened materials

Glass No.*	Salt	Treatment conditions		Mechanism	Flexural strength		Reference
		Temperature (°C)	Time (h)		Before (MPa)	After (MPa)	
(a) *Lithium alumino-silicate glasses*							
18	$NaNO_3$	400	4	$Na^+ \rightleftharpoons Li^+$	–	731	[36]
19	$NaNO_3$	400	4	$Na^+ \rightleftharpoons Li^+$	–	681	[36]
20	$NaNO_3$	400	4	$Na^+ \rightleftharpoons Li^+$	–	669	[36]
21	$NaNO_3$	400	4	$Na^+ \rightleftharpoons Li^+$	–	703	[36]
22	$NaNO_3$	400	4	$Na^+ \rightleftharpoons Li^+$	–	572	[36]
23	$NaNO_3$	385	6	$Na^+ \rightleftharpoons Li^+$	74	470	[44]
23	$NaNO_3$	385	49	$Na^+ \rightleftharpoons Li^+$	74	383	[44]
23	$NaNO_3$	385	97.5	$Na^+ \rightleftharpoons Li^+$	74	336	[44]
24	$NaNO_3$	385	49	$Na^+ \rightleftharpoons Li^+$	–	309	[44]
25	45% Na_2SO_4 + 55% $ZnSO_4$	585	0.25	$Na^+ \rightleftharpoons Li^+$	–	400	[39]
26	$NaNO_3$	404	4	$Na^+ \rightleftharpoons Li^+$	69	669	[42]
(b) *Sodium alumino-silicate glasses*							
27	KNO_3	350	0.17	$K^+ \rightleftharpoons Na^+$	234	579	[47]
27	KNO_3	350	17	$K^+ \rightleftharpoons Na^+$	234	497	[47]
27	KNO_3	400	0.17	$K^+ \rightleftharpoons Na^+$	234	607	[47]
28	KNO_3	400	16	$K^+ \rightleftharpoons Na^+$	65	598	[47]
29	KNO_3	400	16	$K^+ \rightleftharpoons Na^+$	–	476	[48]
30	KNO_3	400	16	$K^+ \rightleftharpoons Na^+$	–	338	[48]
31	KNO_3	400	16	$K^+ \rightleftharpoons Na^+$	–	200	[48]
32	KNO_3	400	16	$K^+ \rightleftharpoons Na^+$	–	600	[48]
33	KNO_3	500	24	$K^+ \rightleftharpoons Na^+$	–	469	[49]
34	KNO_3	500	24	$K^+ \rightleftharpoons Na^+$	–	498	[49]
35	KNO_3	482	4	$K^+ \rightleftharpoons Na^+$	–	650	[51]
36	KNO_3	482	4	$K^+ \rightleftharpoons Na^+$	–	700	[51]
37	KNO_3	400	24	$K^+ \rightleftharpoons Na^+$	–	690	[43]
37	KNO_3	430	1	$K^+ \rightleftharpoons Na^+$	–	552	[43]
37	KNO_3	430	16	$K^+ \rightleftharpoons Na^+$	–	483	[43]
(c) *Mixed lithium-sodium alumino-silicate glasses*							
38	$NaNO_3$	385	49	$Na^+ \rightleftharpoons Li^+$	80–100	503	[44]
39	$NaNO_3$	385	49	$Na^+ \rightleftharpoons Li^+$	80–100	516	[44]
40	$NaNO_3$	385	49	$Na^+ \rightleftharpoons Li^+$	80–100	574	[44]
41	$NaNO_3$	385	49	$Na^+ \rightleftharpoons Li^+$	80–100	858	[44]
42	$NaNO_3$	454	0.5	$Na^+ \rightleftharpoons Li^+$	–	414	[41]
42	$NaNO_3$	496	0.5	$Na^+ \rightleftharpoons Li^+$	–	666	[41]
42	KNO_3	454	1.5	$K^+ \rightleftharpoons Na^+$	–	772	[41]
43	KNO_3	427	1.5	$K^+ \rightleftharpoons Na^+$	–	786	[41]
(d) *Alumina-free alkali silicate glasses*							
44	$NaNO_3$	400	4	$Na^+ \rightleftharpoons Li^+$	62	228	[36]
45	KNO_3	400	16	$K^+ \rightleftharpoons Na^+$	–	235	[47]
46	$NaNO_3$	400	4	$Na^+ \rightleftharpoons Li^+$	55–83	441	[43]
47	$NaNO_3$	400	4	$Na^+ \rightleftharpoons Li^+$	–	366	[43]
(e) *Glass-ceramic compositions*							
48	KNO_3	590	8	$K^+ \rightleftharpoons Na^+$	54	600	[68]
48	52% KCl + 48% K_2SO_4	730	8	$K^+ \rightleftharpoons Na^+$	54	1407	[68]
49	KNO_3	590	8	$K^+ \rightleftharpoons Na^+$	55	862	[68]
49	KNO_3	590	96	$K^+ \rightleftharpoons Na^+$	55	1303	[68]
49	52% KCl + 48% K_2SO_4	730	8	$K^+ \rightleftharpoons Na^+$	55	1379	[68]
50	52% KCl + 48% K_2SO_4	730	8	$K^+ \rightleftharpoons Na^+$	–	1476	[68]
51	90% Li_2SO_4 + 10% K_2SO_4	800	4	$2Li^+ \rightleftharpoons Mg^{2+}$	55	207	[69]
52	90% Li_2SO_4 + 10% K_2SO_4	800	4	$2Li^+ \rightleftharpoons Mg^{2+}$	– 103	379	[69]
53	90% Li_2SO_4 + 10% K_2SO_4	850	8	$2Li^+ \rightleftharpoons Mg^{2+}$	–	1069	[69]
54	52% KCl + 48% K_2SO_4	780	4	$K^+ \rightleftharpoons Li^+$	–	310	[69]
55	Li_2SO_4	1050	24	$2Li^+ \rightleftharpoons Mg^{2+}$	≈ 100	448	[70]
(f) *Glass compositions surface crystallized by chemical methods*							
56	95% Li_2SO_4 + 5% Na_2SO_4	860	0.08	β-eucryptite surface layer	–	638	[22]
57	95% Li_2SO_4 + 5% Na_2SO_4	860	0.25	β-eucryptite surface layer	–	700	[22]

*Specific glass compositions are given in Table VI.

salt bath leads to exchange of Li^+ ions for Mg^{2+} ions ($2\ Li^+ \rightarrow Mg^{2+}$). An increase in the surface density is again achieved, leading to the formation of a surface compressive layer. Strengths up to around 1100 MPa have been achieved using these compositions.

Glass fibres have also been treated by ion-exchange [71]. In this instance, however, an increase in strength was found only on treating unetched fibres, a decrease in strength being noted on treatment of etched material.

A summary of mechanical property data for a variety of chemically strengthened materials is given in Table V. Details of the specific glass compositions reported in both surface crystallization and chemical ion-exchange work are given in Table VI. Further information on chemical strengthening may be found in the paper by Bartholomew and Garfinkel [33].

3.1.2.4. Other surface treatments. Methods of removing surface damage, for example by etching, can

TABLE VI Specific glass-compositions (mol %)

Glass number	Li_2O	Na_2O	K_2O	CaO	TiO_2	MgO	ZnO	B_2O_3	Al_2O_3	SiO_2	P_2O_5	Others
1	11.34	0.31	0.07	–	0.64	–	–	0.09	16.43	70.96	–	0.16 As_2O_3
2	–	–	–	–	–	–	37.63	–	9.88	49.43	1.08	1.98 PbO
3	–	–	–	–	–	–	39.69	–	9.88	49.34	1.09	–
4	–	–	–	–	–	4.97	34.55	–	9.96	49.41	1.11	–
5	–	–	–	2.00	–	–	37.50	–	9.88	49.45	1.08	–
6	–	–	–	–	–	1.99	37.55	–	9.99	49.39	1.08	–
7	–	–	–	–	–	1.96	38.05	–	10.03	49.96	–	–
8	–	–	–	–	–	–	31.64	–	11.22	57.14	–	–
9	4.60	–	–	–	–	–	33.78	–	6.74	54.88	–	–
10	4.94	–	–	–	–	–	34.20	–	10.13	50.73	–	–
11	4.64	–	–	6.17	–	–	32.08	–	9.51	47.60	–	–
12	–	1.17	–	–	–	–	40.00	–	10.00	48.83	–	–
13	–	–	–	–	–	–	40.05	1.05	10.01	48.89	–	–
14	4.73	–	–	–	–	–	37.05	–	9.69	48.53	–	–
15	–	–	–	–	0.91	–	40.10	–	10.02	48.97	–	–
16	–	–	–	24.00	–	–	20.30	–	9.60	46.10	–	–
17	–	–	–	63.16	–	–	–	–	36.84	–	–	–
18	18.00	–	–	–	–	–	–	–	22.00	60.00	–	–
19	18.00	–	–	–	–	–	–	–	26.00	56.00	–	–
20	22.00	–	–	–	–	–	–	–	18.00	60.00	–	–
21	22.00	–	–	–	–	–	–	–	22.00	56.00	–	–
22	16.34	–	–	–	–	–	9.07	–	20.01	54.58	–	–
23	29.60	–	–	–	–	9.96	–	–	9.90	49.39	1.15	–
24	30.30	–	–	–	–	8.12	–	–	10.11	50.28	1.19	–
25	16.67	–	–	–	–	–	–	–	16.67	66.66	–	–
26	11.03	0.47	0.06	–	0.62	–	–	0.36	16.19	71.08	–	0.19 As_2O_3
27	–	13.71	0.97	6.17	–	4.52	–	–	1.31	72.65	–	0.67 BaO
28	–	11.33	2.53	0.24	–	–	–	1.90	11.69	72.31	–	–
29	–	15.81	–	5.30	–	5.16	–	–	0.58	73.15	–	–
30	–	14.40	–	9.55	–	3.69	–	–	0.58	71.78	–	–
31	–	3.98	–	–	–	–	–	10.63	1.21	84.18	–	–
32	–	17.29	1.42	2.39	3.77	–	–	1.92	12.48	60.73	–	–
33	–	13.35	2.47	0.23	0.65	5.93	–	–	10.78	66.59	–	–
34	–	13.53	2.47	0.23	–	5.92	–	–	10.76	67.09	–	–
35	–	21.83	2.39	–	–	–	4.62	–	11.06	49.41	–	2.75 ZrO_2
36	–	20.95	2.30	–	–	3.52	4.49	–	12.44	46.68	7.62	2.00 ZrO_2
37	–	15.00	2.00	–	–	–	6.50	4.50	1.00	70.00	–	1.00 PbO
38	20.76	4.82	–	–	–	10.35	–	2.43	10.29	51.35	–	–
39	17.68	4.26	–	–	–	10.92	–	3.79	11.51	50.81	1.03	–
40	17.86	4.31	–	–	–	11.03	–	3.84	11.63	51.33	–	–
41	18.72	2.26	–	–	–	19.42	–	1.20	10.42	47.00	0.98	–
42	11.61	12.22	–	–	–	–	2.54	–	17.96	50.84	4.83	–
43	11.03	7.38	–	–	–	–	1.61	4.70	12.57	61.35	1.36	–
44	25.00	–	–	–	–	–	–	–	–	75.00	–	–
45	–	14.81	–	–	–	–	–	8.79	–	76.40	–	–
46	17.82	–	–	–	–	–	–	–	–	72.10	–	9.93 ZrO_2 + 0.15As_2O_3
47	16.08	–	–	–	–	–	–	–	–	76.46	–	7.31 ZrO_2 + 0.15As_2O_3
48	–	17.00	2.37	–	6.68	–	–	–	22.16	51.53	–	0.26 As_2O_3
49	–	13.87	5.85	–	6.80	–	–	–	22.48	50.74	–	0.26 As_2O_3
50	–	11.42	6.86	–	6.30	–	–	–	20.82	54.36	–	0.24 As_2O_3
51	5.15	–	–	–	–	6.12	1.51	–	12.70	72.36	–	2.00 ZrO_2 + 0.16 As_2O_3
52	4.08	–	–	–	–	9.09	–	–	13.18	71.17	–	2.48 ZrO_2
53	–	–	–	–	7.46	19.23	–	–	18.72	54.59	–	–
54	4.08	–	–	–	–	6.83	–	–	11.69	75.26	–	1.99 ZrO_2 + 0.15 As_2O_3
55	3.42	–	–	–	–	4.73	–	–	19.24	69.51	–	3.10 ZrO_2
56	2.49	12.00	–	–	5.25	–	–	–	15.72	64.37	–	0.17 As_2O_3
57	7.09	7.62	–	–	4.89	–	–	–	14.06	66.18	–	0.16 As_2O_3

promote very large, although transient, increases in mechanical strength of brittle materials. More practical methods include cladding the material with a more resiliant coating, or cladding with a higher thermal expansion material to promote the formation of a surface compressive layer. These methods are not in general, however, as versatile as the methods of thermal or chemical strengthening. Cladding of glass articles with a glass coating of lower thermal expansion has been practised for a number of years [72]. More recent work by James [73] has concentrated on coating glass rods of various compositions with low thermal expansion borate glass. Using this low viscosity glass, consistent, even coatings $\approx 200\,\mu\text{m}$ thick were readily achieved. Strength increases were noted for abraded rods from around 110 to 350 MPa. Glass fibres have also been strengthened by cladding. For example, Krohn and Cooper [74] produced borosilicate glass fibres coated with silica by the drawing down of a silica coated glass rod. For a fibre of outside diameter about $180\,\mu\text{m}$ with a core to cladding ratio of 2/3, a strength increase for abraded fibres from about 155 to 290 MPa was noted. Krohn [75] also examined the influence of thermal expansion mismatch, $\Delta\alpha$, between different glass cores and claddings; a maximum surface compression of about 320 MPa was found for a system of $\Delta\alpha \approx 8.5 \times 10^{-6}\,{}^{\circ}\text{C}^{-1}$. Enhanced strength attributed to surface compression has also been noted for glass articles, including fibres, coated with a thin layer of titania [76–78]. Similarly, coating with tin oxide improves the mechanical properties [79]. Finally, coating with polymeric materials has been used for many years in the glass fibre industry for improving the resistance of glass fibres to surface damage during handling and storage [80].

3.1.3. Stress profile determination

The stress profile of surface modified glasses is an important property which controls not only the ultimate strength of the material, but also the way in which it fractures. Stress profiles in optically transparent materials may be measured by conventional photoelastic methods [81], by the scattered light technique [81, 82], or by progressively removing surface layers by etching and then measuring the resultant dimensional changes [83]. This latter method is also suitable for measuring the stress profiles of optically opaque materials. An alternative method for measuring transparent materials, which is more suited to the measurement of stress profiles in thin, chemically strengthened glasses where the stress gradients are relatively high, has been developed by Bradshaw [84]. This method combines the scattered light technique with etching. It involves the scattering of light from a finely collimated laser beam passed through the central plane of the sample and plane polarized at 45° to the plane of the sample. Due to the birefringence of the glass when stressed, this beam splits into two components and gives rise to interference fringes when viewed at 45° to the surface of the glass. From a knowledge of the fringe separation, b, and the stress optical coefficient, C, of the glass, a value for the centre tension, σ_c, can be derived using the following expression

$$b = \lambda/\sigma_c C \tag{5}$$

where λ is the wavelength of light employed.

The glass is then etched in an aqueous solution of $HF + H_2SO_4$ to remove some of the surface. After removal of a thin surface layer, the new, reduced centre tension is measured. This process is then repeated a convenient number of times until zero or near-zero centre tension is achieved. An excellent example of the variation in fringe separation with thickness change, taken from the work of Bradshaw [84], is shown in Fig. 6. The stress profile is subsequently derived from the relationship between the thickness change and centre tension change. This may be accomplished by plotting a graph of thickness change against centre tension and measuring the gradient at successive points to calculate the stress profile using the relationship

$$\sigma = G(t/2 - L) + \Delta\sigma_c \tag{6}$$

where σ is the stress in the layer removed, G the gradient of the curve, t the original thickness of the sample, L the thickness loss per side, and $\Delta\sigma_c$ the total decrease in centre tension taken from the start of the etching treatment.

In general, the stress profiles measured experimentally differ somewhat from the idealised profile for a chemically strengthened glass shown in Fig. 2. Very often, the maximum compressive stress is found not at the surface, but at some distance within the glass

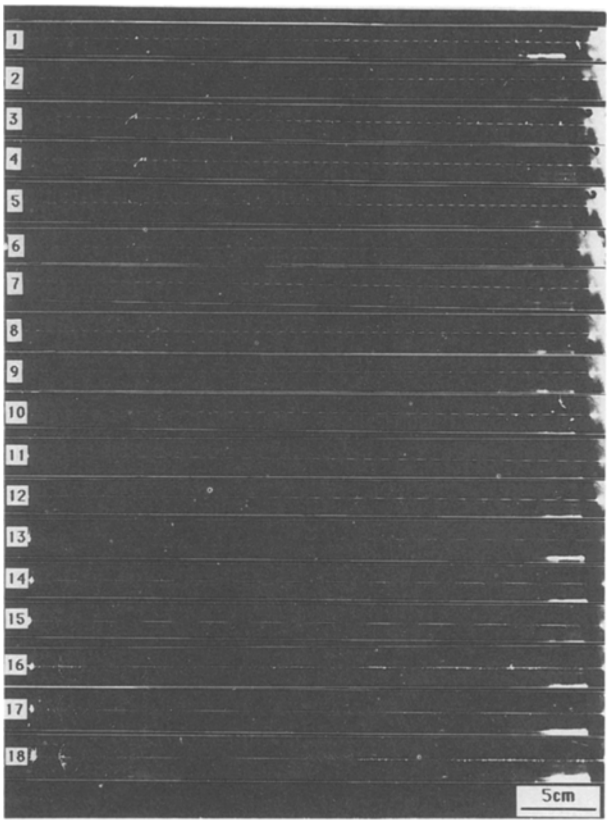

Figure 6 Variation in fringe separation with decrease in thickness for Corning 0319 chemically strengthened glass; after [84]. (1 is as-received material with t = 1.3 mm; 2 to 18 are after progressively etching away some of the surface with t = 0.7 mm for 18.)

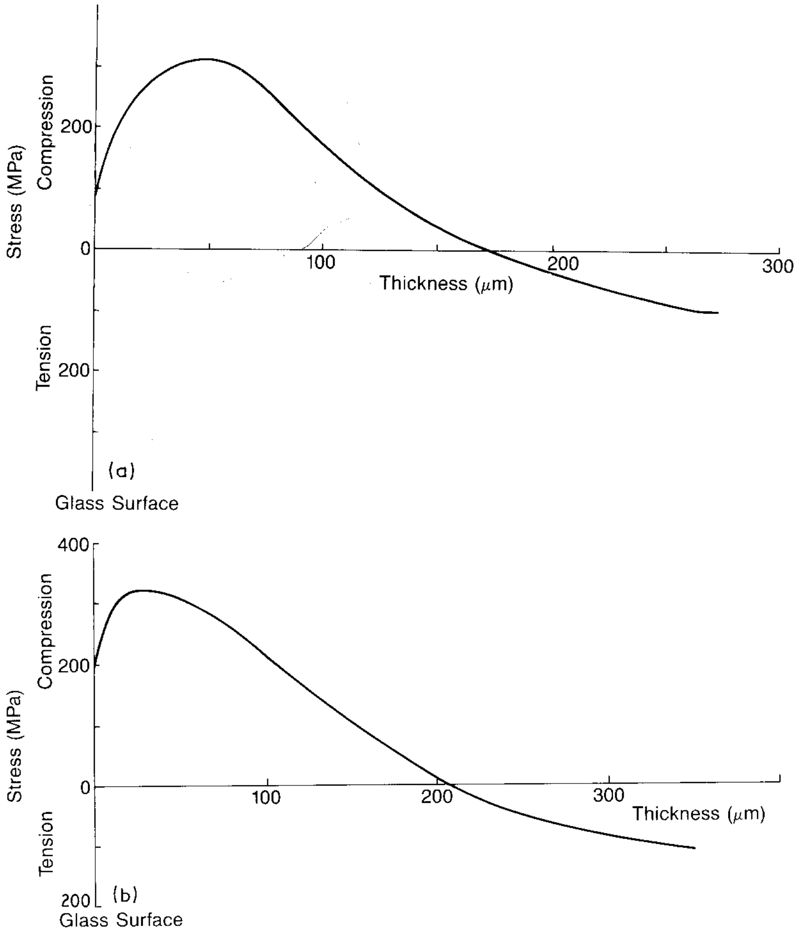

Figure 7 "Relaxed" stress profiles of chemically strengthened glasses: (a) lithium magnesium alumino-silicate glass; after [44], (b) sodium alumino-silicate glass (Corning 0319); after [84].

interior, as shown in Fig. 7a for a Li_2O–Na_2O–MgO–Al_2O_3–SiO_2 glass treated in $NaNO_3$ [44, 45], and in Fig. 7b for a commercially available Na_2O–Al_2O_3–SiO_2 glass [84]. This type of effect may be related to the influence of thermal stress relaxation of the glass during treatment, particularly when treatment is carried out at temperatures approaching T_g. Alternatively, it may be related to differences in thermal expansion between the bulk glass and the ion-exchanged layer, the latter possessing a higher thermal expansion than that of the bulk material. In the extreme case, this expansion mismatch may be sufficiently large to create tension in the outermost layers of the glass, rather than compression, and this may lead to crazing and spalling of the glass surface, as has been observed by Donald and Hill [44, 45] for a Li_2O–MgO-Al_2O_3-SiO_2 glass. This effect is shown in Fig. 8. Further stress profile data for a variety of thermally strengthened and chemically strengthened glasses have also been reported by a number of authors, employing some of the techniques outlined above [38, 42, 48, 51, 84–86].

3.1.4. Fracture behaviour and life prediction studies of surface modified glasses

All these surface methods just described increase the strength of brittle oxide glasses, and their strain to failure. In all instances, however, ultimate failure

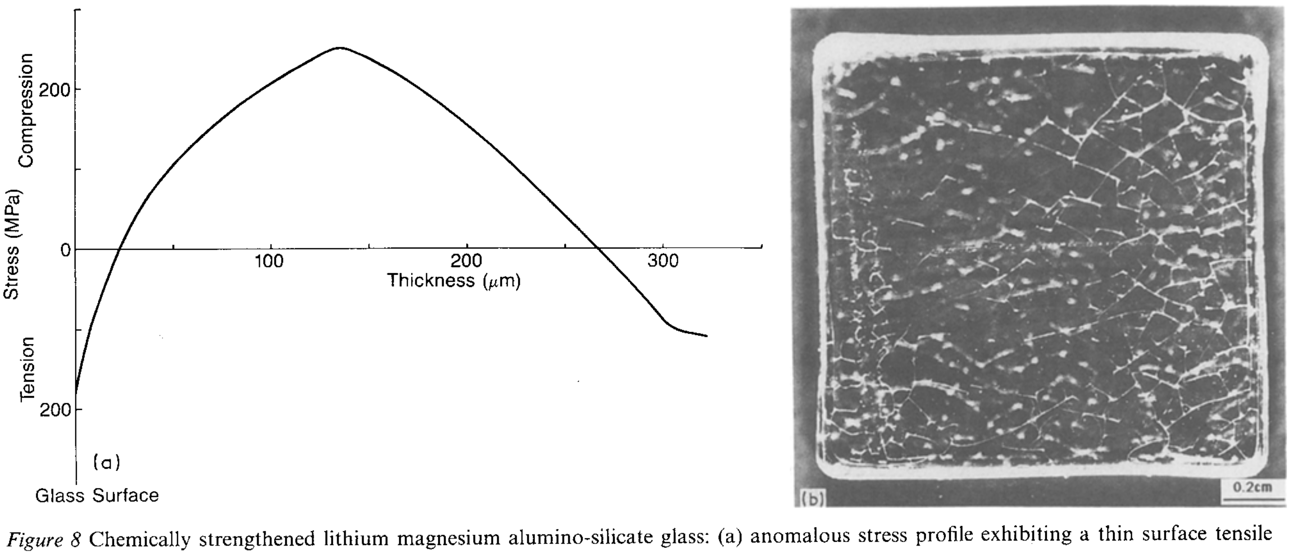

Figure 8 Chemically strengthened lithium magnesium alumino-silicate glass: (a) anomalous stress profile exhibiting a thin surface tensile zone, (b) surface crazing effect caused as a result of this tensile layer; after [44].

is still catastrophic, the materials behaving as fully elastic solids, and fracture toughness is not improved upon significantly.

The actual fracture behaviour of surface modified glasses has been studied extensively in terms of examining the short time failure characteristics of these materials under dynamic loading conditions. Typical short time fracture behaviour, as a function of treatment time, for a Li_2O–MgO–Al_2O_3–SiO_2 glass of thickness of about 1.3 mm treated in $NaNO_3$ at 385 °C is illustrated in Fig. 9, after the work of Donald and Hill [44]. The decrease in franged particle size with increasing treatment time is a consequence of the increasing magnitude of the internal tensile stress and correspondingly higher internal strain energy. There has been much less work in the important areas of impact damage and life assessment studies. This is partly because the relatively high stress gradients associated with these materials makes analysis by conventional fracture mechanics techniques very difficult. In one early study, however, Barsom [87] discussed fracture behaviour in terms of the stored elastic strain energy and the elastic energy release rate during crack extension. Useful fracture mechanics analyses have also been carried out by Lawn and Marshall [88] both for thermally and chemically strengthened glasses. The spontaneous failure or franging of surface modified glasses has been noted in some cases [87–91]. Bakioglu *et al.* [89] have shown, via a fracture mechanics analysis, that this effect could be caused by the slow growth of subcritical surface cracks, but only if the original critical flaw extends almost into the tensile zone. Hsiao [90] noted that NiS inclusions in thermally strengthened glasses could also lead to spontaneous failure due to a phase transformation involving a volume change occuring within the NiS as

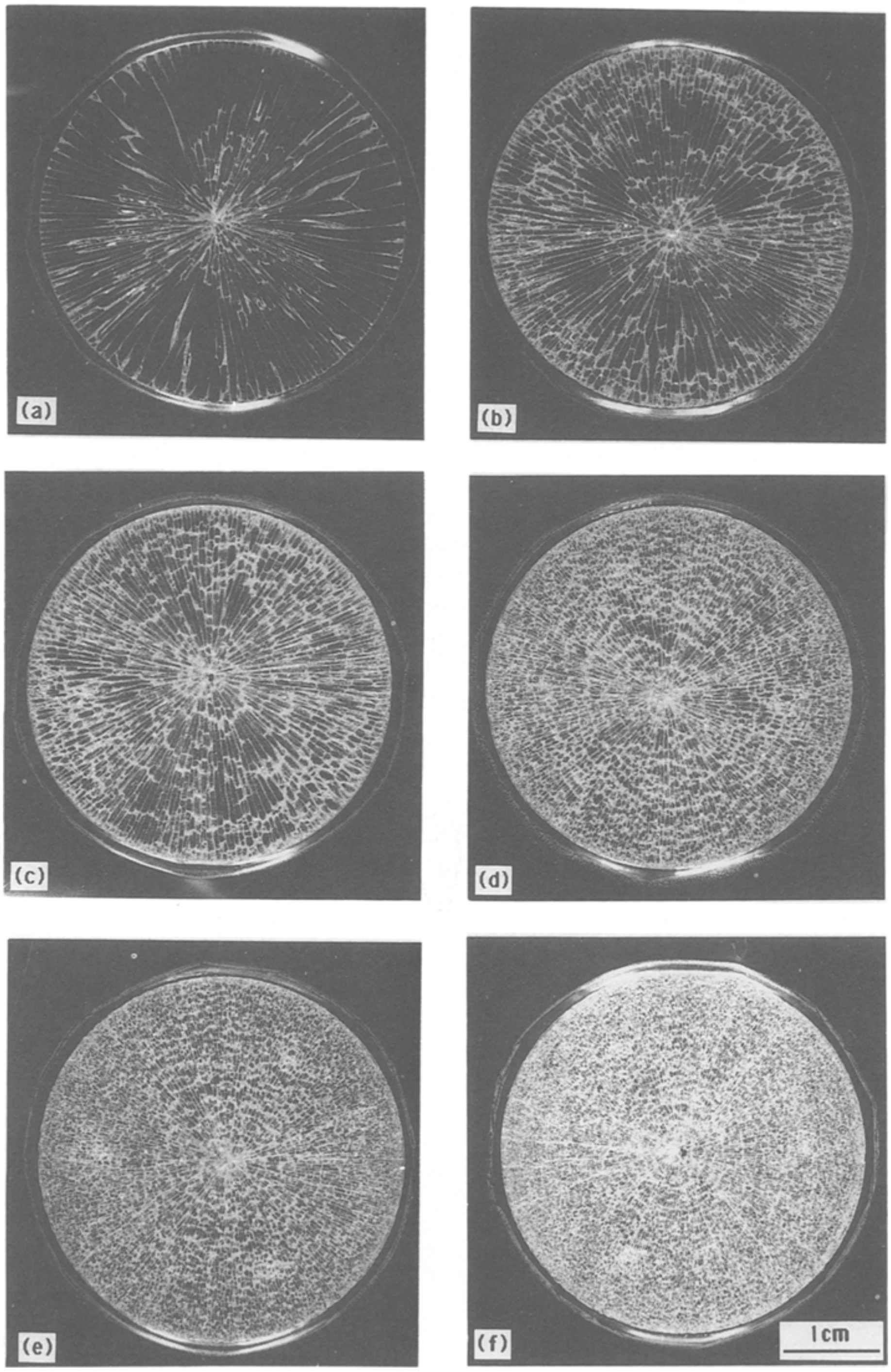

Figure 9 Fracture behaviour of chemically strengthened lithium magnesium alumino-silicate glass discs ≈ 1.2 mm thick as a function of the treatment time in sodium nitrate at 385° C; after [44]. For (a) t = 6 h, (b) t = 17 h, (c) t = 25 h, (d) t = 49 h, (e) t = 65 h, (f) t = 97.5 h.

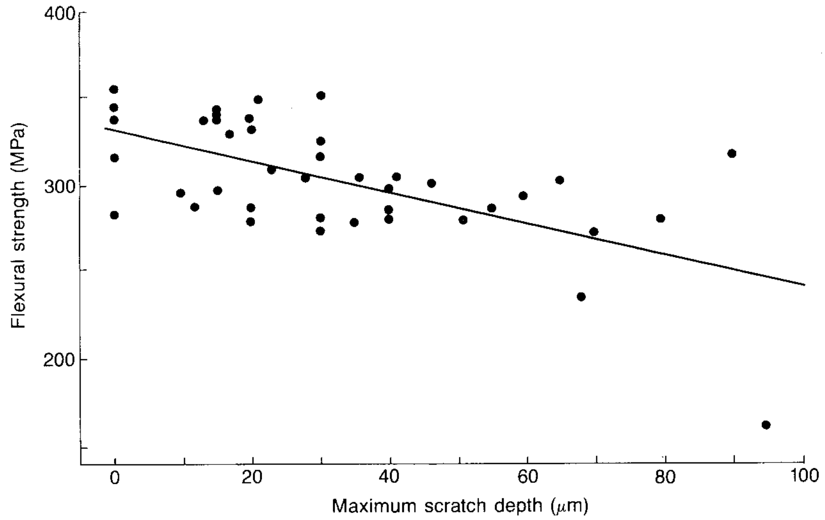

Figure 10 Modulus of rupture in four-point bending of Corning 0319 chemically strenghthened glass as a function of scratch depth; after [96].

a function of time. Chang and Chou [91] have also examined the failure of thermally strengthened glass at stresses less than their normal failure stress. In addition, impact fracture behaviour has been studied to some degree for these materials, particularly in light of their role in aircraft transparencies [92–95]. Fracture studies of damaged chemically strengthened glasses have not been widely reported. In one study, however, Donald and Metcalfe [96] found that the short-term strength of Corning 0319 chemically strengthened glass containing surface scratches decreased with increasing scratch depth, as illustrated in Fig. 10, and Swain *et al.* [97] have also attempted to predict the resistance of thermally strengthened glasses to surface damage.

3.2. Bulk methods of improving strength and toughness

In addition to surface methods for improving mechanical strength, a number of bulk methods have also been utilized in attempts to improve the strength and other properties of oxide glasses. A number of the bulk methods are particularly aimed at improving the fracture toughness of brittle materials. General methods for improving strength and/or toughness are outlined below.

3.2.1. Bulk crystallization to produce glass–ceramics

Glass–ceramics are generally significantly stronger than their glassy counterparts, and exhibit many other useful properties (e.g. [98–102]). The increased strength is attributable to a combination of factors, including microstructural limitation of the maximum size of Griffith-type flaws present in the material. The strength may also be high compared to many conventional ceramics, and this too is ascribed to microstructural features, including very small grain size (significantly smaller than most ceramics produced by conventional techniques, including sintering and hot-pressing), and to the complete absence of internal defects such as grain-boundary porosity and inclusions. The strength of a glass–ceramic material normally increases with increasing crystallization temperature, reaching a maximum over a particular temperature range, as illustrated in Fig. 11. On increasing the crystallization temperature further, strength may then start to decrease; this is due to a combination of mechanisms, including grain growth or the formation of crystalline phases of thermal expansion markedly different to that of the matrix, which results in the creation of high internal stresses [103–107]. Microhardness has also been noted to undergo similar

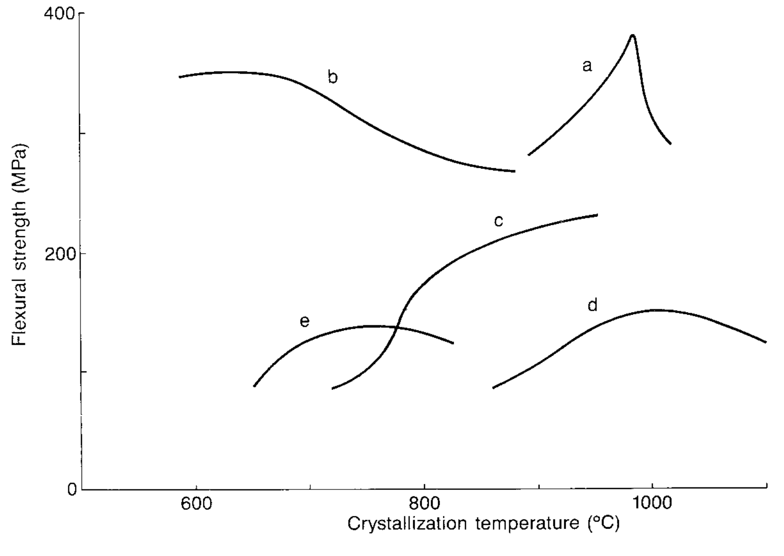

Figure 11 Strength of glass–ceramic materials as a function of crystallization heat treatment temperature (a magnesium alumino-silicate glass–ceramic nucleated with ZrO_2; after [103], b lithium silicate glass–ceramic nucleated with P_2O_5; after [104], c lithium alumino-silicate glass–ceramic nucleated with P_2O_5, after [105], d magnesium alumino-silicate glass–ceramic nucleated with P_2O_5; after [106], e lithium zinc silicate glass–ceramic nucleated with P_2O_5; after [107]).

behaviour (e.g. [108–111]. The toughness of a glass–ceramic is also greater than that of the parent glass, due to the crack impeding properties of grain boundaries, but it is still very considerably lower than that of a ductile metal. Hence, glass–ceramics, although generally mechanically stronger than their glassy counterparts, are still brittle solids, exhibiting classical brittle behaviour and catastrophic failure characteristics.

3.2.2. Particle reinforcement

Strengthening by incorporation of a fine dispersion of second-phase particles has long been utilized for metallic systems. The particles may be produced *in situ* by precipitation of a secondary phase (precipitation or age hardening), or may be added directly by powder metallurgy routes (dispersion strengthening). Dispersion strengthening and precipitation hardening techniques may also be utilized for ceramic materials. Since dislocation mobility is already extremely low in ceramics (at ambient temperatures), and dislocations as conventionally defined do not exist in glasses, particle dispersions would not be expected to contribute very significantly to an increase in strength. Significant strengthening has, nevertheless, been observed for certain particle reinforced ceramic systems, including glass reinforced with oxidized nickel microspheres less than or equal to $25\,\mu$m in diameter [112], alumina containing molybdenum dispersions of submicrometre particle size [113], various materials containing zirconia dispersions [114], and a number of glasses containing aluminium particles [115, 116]. Later work on zirconia and zirconia-containing ceramics has led to a new class of strong, tough materials, the "transformation-toughened" ceramics, and this is discussed more fully later. Increases in strength have also been reported for glasses containing alumina and tungsten dispersions [117, 118]. Conversely, decreases in strength have been noted for many systems, depending on such factors as dispersoid size and shape, and process parameters [119–121].

The increase in strength noted for some of the particle reinforced ceramic systems has been attributed to a number of different mechanisms. For example, it has been suggested that strengthening may be due to the fine dispersions limiting the size of Griffith-type flaws, thereby raising the stress required to initiate or propagate a crack. Strengthening may also result from line-tension effects due to particles initially pinning a propagating crack front and causing it to bow out between the obstacles [122, 123], in a similar manner to that observed on an atomic scale for dislocations in crystalline materials. In addition, if particles of higher elastic modulus than that of the matrix are employed, and strong particle–matrix bonding exists, stress transfer from the matrix to the reinforcing phase will occur, and some of the load will be shared by the higher modulus particles. This means that a higher stress can be achieved before the failure strain of the matrix is reached, resulting in a stronger material. In ductile particle reinforced systems ligament formation, in which cracks do not circumvent the particles but evoke plastic deformation and rupture of the particles instead, may lead to enhanced fracture toughness [124]. In the case of crystalline ceramics, including glass–ceramics, fine dispersions may also inhibit grain growth during fabrication or use, thereby giving a grain size strengthening effect.

Under suitable conditions, the effect of thermal expansion mismatch, $\Delta\alpha$, between matrix and dispersoid may be used to advantage, and promote strengthening of the matrix. If the value of $\Delta\alpha$ is negative ($\Delta\alpha = \alpha_{\text{matrix}} - \alpha_{\text{dispersoid}}$), and the particle–matrix interface can support the resulting radial tensile stresses on cooling from the fabrication temperature, the surrounding matrix will be subjected to tangential compressive stresses, and the matrix may be strengthened. If, on the other hand, $\Delta\alpha$ is positive, induced tangential tensile stresses may weaken the matrix and, in the limiting case, localized failure of the matrix may occur giving rise to a microcracked system. The resulting radial and tangential stresses α_r and α_t, respectively, may be assessed using Selsing's formula [125]

$$
\begin{aligned}
-\sigma_r &= 2\sigma_t \\
&= \Delta\alpha\,\Delta T/\{([1 + \nu_m]/2E_m) + ([1 - 2\nu_p]/E_p)\}
\end{aligned} \tag{7}
$$

where, ΔT is the difference between fabrication and ambient temperature, ν_m Poisson's ratio of the matrix, ν_p Poisson's ratio of the dispersed phase, E_m Young's modulus of the matrix, and E_p Young's modulus of the dispersoid.

If $\Delta\alpha$ is positive, matrix microcracking is expected when the value of σ exceeds the tensile strength of the matrix, and microcracking has indeed been observed in a number of cases. For example, in a glass–alumina system of $\Delta\alpha \approx +7 \times 10^{-6}\,{}^\circ\mathrm{C}^{-1}$ [126], and in glass–thoria [120], MgO–W [127], and glass–glass composites of positive $\Delta\alpha$ [128]. On the other hand, when $\Delta\alpha$ is negative, strengthening is predicted for suitable bonded systems, and this has been observed in practice for some glass–nickel systems, cited earlier [112], and for a number of glass–alumina and glass–zirconia composites [126]. If the value of $\Delta\alpha$ is too negative, however, the particle–matrix interface or the surrounding matrix may not be strong enough to withstand the induced radial tensile stresses, and decohesion will occur leading to a loss in strength, as has been observed, for example, for a glass–nickel system with $\Delta\alpha \approx -12 \times 10^{-6}\,{}^\circ\mathrm{C}^{-1}$ [121], and for a glass–thoria composite of particle size greater than a critical value [120].

In general, none of the above methods of particle reinforcement lead to really practical increases in fracture toughness, although certain particle reinforced aluminium–glass [115] and Fe-Ni–Co alloy–glass [129] systems have been found to exhibit K_{Ic} values in the range 5 to $7\,\mathrm{MPa\,m^{1/2}}$. These materials remain prone to catastrophic failure, however, and fail at relatively low fracture strains. The expanding field of transformation strengthening or toughening is, on the other hand, providing some useful materials, exhibiting both high mechanical strength and moderate toughness.

The phenomenon of transformation toughening has arisen due to the utilization of rapid stress-induced structural transformations that involve molar volume and/or shape changes. In principle, the concept should be applicable to a number of structural transformations in various ceramic materials, but has so far only been demonstrated effectively for zirconia. On cooling zirconia to room temperature from around 1200 °C, the tetragonal to monoclinic phase transformation would normally occur. If, however, the zirconia is finely divided, or is incorporated into a matrix where it is subjected to a constraining pressure (due to thermal expansion mismatch between matrix and particle, with $\alpha_{\text{matrix}} > \alpha_{\text{particle}}$) the zirconia can be maintained in a metastable tetragonal form. When a dispersion of such particles is present in a ceramic matrix it can act to toughen the matrix, by impeding the propagation of cracks through the matrix. The toughening mechanism is due to the volume change accompanying the stress-induced transformation of the metastable tetragonal particles to the monoclinic form in the presence of a propagating crack. Tensile stresses are generated in the vicinity of a propagating crack. If these stresses are high enough, the constraint on the adjacent particles is removed, and the zirconia transforms spontaneously by a diffusionless martensitic-type reaction to the stable monoclinic form. The accompanying volume change creates a compressive stress field in the vicinity of the propagating crack, and this acts to close up the crack tip, so hindering its continued propagation.

The zirconia particle size is important in determining the resultant properties of a zirconia dispersion strengthened material. If the particles are too small, they will not transform, whilst if they are too large, they will transform spontaneously. There is, therefore, a critical particle size range for a given system, above or below which significant toughening is not achieved. This critical size depends on a number of factors, including the magnitude of the constraint imposed by the matrix on the particles, and the chemical composition of the zirconia. It is possible, for example, to alloy zirconia with other oxides that will stabilize the cubic and tetragonal phases. For these materials larger particle sizes can be tolerated without spontaneous transformation to the monoclinic form occurring.

The method of transformation toughening was first successfully applied by Garvie *et al.* [130] in 1975, and since then considerable effort has been devoted by various research groups (e.g. Porter and Heuer [131, 132], Claussen [133, 134], Lange [135]) to finding new, improved formulations. Some of the detailed work has been reviewed recently by Heuer [132]. One of the most widely studied systems has been alumina containing tetragonal zirconia particles. The most successful systems have been found to contain $\approx 15\%$ zirconia of 1 to 2 μm particle size, and exhibit fracture toughness values, K_{Ic}, of the order of $10\,\text{MPa}\,\text{m}^{1/2}$, coupled with a flexural strength in excess of 400 MPa [136]. Other matrices have also been utilized with limited success, including zinc oxide, silicon carbide and silicon nitride [137].

Investigations have also centred around the formation of partially stabilized zirconia.It has been found, as mentioned earlier, that alloying zirconia with certain other oxides, in particular MgO, CaO and Y_2O_3, can stabilize the cubic or tetragonal zirconia phase. If suitable compositions are quenched from a high temperature, a single cubic phase material results. These materials can then subsequently be aged to "precipitation harden" the zirconia matrix by the development of a fine dispersion of tetragonal zirconia crystals in the cubic zirconia matrix. These particles then act to toughen the matrix by the transformation toughening mechanism. If, however, the materials are overaged, the particles transform into the monoclinic phase and little or no toughening results.

Although most of the work to date has centred on transformation toughening of "conventional" crystalline ceramic materials, e.g. alumina and zirconia, a limited amount of work has been reported on the toughening of glasses and glass-ceramics, and it would appear that there is considerable scope for further work in this area. For example, Fagherazzi *et al.* [138] reported the preparation of a Na_2O–Al_2O_3–ZrO_2–SiO_2 glass–ceramic containing tetragonal and monoclinic zirconia crystals, although the full potential of the transformation toughening process does not seem to have been exploited. Keefer and Michalske [139] have reported the preparation of silicate glass–ceramics containing up to around 30% zirconia, in which small crystals of tetragonal zirconia can be precipitated out on careful heat treatment. Glass–ceramics based on the 3 ZrO_2–2 SiO_2 system have also been prepared by Nogami and Tomozawa [140] using a sol–gel technique. A K_{Ic} fracture toughness value of around $5\,\text{MPa}\ \text{m}^{1/2}$ was observed for a sample containing a fine dispersion of tetragonal zirconia crystals ≈ 40 nm in size. Mechanical property data for some of these materials are summarized in Fig. 12 and Table VII.

3.2.3. Fibre reinforcement

The use of high modulus fibres in a lower modulus matrix is a well known and routinely practised technique for increasing the strength of, for example, organic polymeric materials. The general theory of fibre reinforcement indicates that significant strengthening will only occur, however, if the elastic modulus of the fibres is considerably greater than that of the matrix, and if tensile stresses can be transmitted to the fibres. If fibres of lower modulus are employed, the ultimate failure stress will be reduced because the matrix, rather than the fibres, will carry a greater proportion of the applied load.

Stresses may be transmitted to the fibres by plastic or elastic deformation of the matrix. In the absence of internal stresses, the strength, σ_c of a continuous fibre reinforced composite may be estimated by the simple rule of mixtures criterion, assuming the strains in each component are equal, as

$$\sigma_c = \sigma_{fu} V_f + \sigma_m V_m \tag{8}$$

or as

$$\sigma_c = \sigma_f V_f + \sigma_{mu} V_m \tag{9}$$

where σ_{fu} is the ultimate failure strength of the fibre, V_f the volume fraction of fibre, σ_m the matrix stress

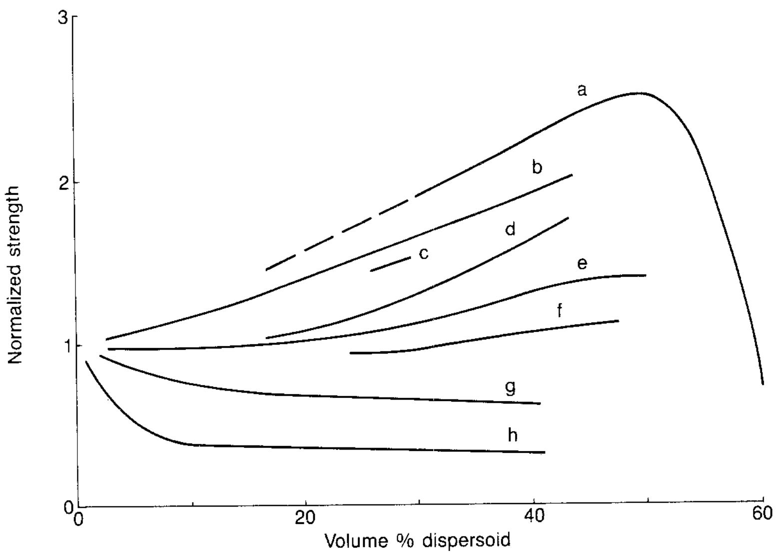

Figure 12 Normalized strength of particle-reinforced glass and glass–ceramic matrix composites as a function of dispersoid concentration: (a sodium borosilicate glass + 3 to 13 μm diameter tungsten microspheres; after [118], b sodium calcium silicate glass + $\leqslant 40\,\mu$m aluminium-alloy microspheres; after [116], c sodium calcium silicate glass + 30 μm diameter oxidized nickel microspheres; after [112], d sodium borosilicate glass + 15 μm diameter alumina particles; after [117], e as a but containing 50 μm diameter microspheres, f as d but containing 60 μm diameter particles, g glass + zirconia particles; after [119], h glass + 74 to 105 μm diameter nickel microspheres; after [121].)

at the fibre failure strain, V_m the volume fraction of the matrix phase, σ_f the fibre stress corresponding to the matrix failure strain, and σ_{mu} the ultimate failure strength of the matrix, depending on which component fails first, and assuming that composite failure occurs immediately following failure of one of the components.

For discontinuous reinforcement, the ultimate strength of a given fibre can only be utilized if it lies parallel to the tensile axis, and if its length exceeds a critical length, defined as the minimum fibre length in the composite which can just be loaded to its failure stress. If randomly orientated fibres are employed, the proportion of fibres capable of being loaded to their fracture stress will be reduced, and hence the ultimate strength of the composite will be lower than that of an equivalent aligned system. Suitable "efficiency" factors have been derived to take into account the effect of fibre orientation and length, although a knowledge of the critical length is required in order to predict the length efficiency factor (e.g. Krenchel [141], Laws [142]).

On the basis of the above general theory of fibre reinforce-ment, there would seem to be only very limited scope for strengthening a high modulus brittle ceramic material, which exhibits neither plastic flow nor extensive elastic deformation, by the fibre reinforcement mechanism.

The incorporation of fibres into relatively high modulus ceramic materials was, however, originally carried out specifically in order to increase the fracture toughness, rather than the strength, of these brittle materials. The early aim was, therefore, to produce a composite material which combined the advantages of a ceramic, e.g. high strength at elevated temperatures, low density, high thermal stability and oxidation resistance, high mechanical hardness and abrasion resistance, and good electrical insulating properties

TABLE VII Properties of particle-reinforced glass and glass–ceramic matrix composites

Matrix	Type	Particle Diameter (μm)	Volume fraction	Composite flexural strength			Reference
				Absolute (MPa)	Normalized	Fracture toughness (MPa m$^{1/2}$)	
SBS glass	Al_2O_3	60	0.475	117	1.16	–	[117]
SBS glass	Al_2O_3	21	0.475	163	1.40	–	[117]
SBS glass	Al_2O_3	15	0.423	174	1.49	–	[117]
SBS glass	W	20	0.50	57	1.16	–	[118]
SBS glass	W	3–13	0.50	155	2.72	–	[118]
LSAS glass	Al	100–130	0.20	–	–	7.0	[115]
SBS glass	Ni	25	0.20	83	1.56	–	[112]
SAS glass	Ni	25	0.20	106	1.56	–	[112]
C7052	Fe–Ni–Co alloy (kovar)	44–75	0.68	–	–	5.5	[129]
ZS glass–ceramic	ZrO_2	0.04	–	–	–	4.8	[140]
SCS glass	Al	53	0.40	118	1.69	–	[116]
SCS glass	Al alloy	42	0.40	161	2.18	–	[116]
Bioactive SCPS glass	Al alloy	40	0.40	86	1.51	–	[116]

SBS—sodium borosilicate;
LSAS—lithium sodium alumino-silicate;
SAS—sodium alumino-silicate;
C7052—Corning Code 7052 borosilicate sealing glass;
ZS—zirconium silicate; SCS—sodium calcium silicate; SCPS—sodium calcium phospho-silicate

etc, with a high resistance to catastrophic failure. It was the lack of toughness that early work tried to improve upon, by addition of fibres to act as barriers to crack propagation, thereby preventing the familiar catastrophic failure behaviour associated with these materials.

Fibres are intuitively effective at providing barriers to crack propagation and thereby increasing the fracture toughness of a material, although their precise role is complex and difficult to describe or quantify fully. The concept of fibre reinforcement is not new. Straw, for example, has been used to produce reinforced building bricks for several thousand years, and is still in use today in many parts of the world. It was only in the 1960s, on the other hand, that serious attempts were made to produce high quality, high performance fibre reinforced ceramics, driven by the immense potential of these materials in aerospace-type applications, and in particular including gas turbine components.

There are a number of mechanisms by which the total work of fracture may be raised. One is to increase the effective crack propagation area by providing planes of weakness within the material, in a direction parallel to the tensile axis, along which a propagating crack may be deflected, thereby effectively blunting crack tips. Aveston has shown [143] that very high values for the work of fracture are possible by this mechanism. If, on the other hand, the fibre–matrix bond is sufficiently strong, a crack may propagate relatively unimpeded through the composite, and the work of fracture will be low. If discontinuous fibres are employed of length, l, less than the critical length, l_c, the fibres will not be loaded to their fracture stress and they must be withdrawn from the matrix as the fracture planes separate. It has been shown by Cottrell [144], that the contribution due to pull-out can be very significant, and the maximum value $\gamma p_{\max}$, is obtained for $l = l_c$, when

$$\gamma p_{\max} = V_f \tau l_c^2/12r \qquad (10)$$

where τ is the interfacial shear stress resisting pull-out, and r the fibre radius. If the fibre length $l > l_c$, some pull-out is still observed, since many of the fibres will intersect the crack plane within a distance $l_c/2$, and hence a fraction l_c/l of the fibres will not be loaded to their fracture stress, and must pull-out as the planes separate. The fact that pull-out effects have also been observed for many continuous brittle-fibre systems has been attributed to the statistical distribution of strength along these fibres, allowing fracture of many fibres to occur at positions away from the fracture plane.

In the case of ductile reinforcing fibres, a large contribution to the fracture toughness of the composite may be provided by plastic flow and rupture of the fibres. For fibres of length, $l > l_c$, the contribution, γ_r, due to fibre rupture will be

$$\gamma_r = V_f \gamma_f (l - l_c/l) \qquad (11)$$

where γ_f is the fibre rupture energy. Unfortunately, the high work of fracture of metals cannot always be utilized to full advantage because wire embrittlement may occur for some metals during fabrication; for example, due to chemical reaction with the matrix. In these cases high values for fracture toughness may still be achieved, nevertheless, by the pull-out mechanism.

If the fibres are randomly orientated, many fibres will cross the fracture plane obliquely and will be subjected to a bending moment. In the case of brittle fibres, this will lower the applied tensile stress required to fracture the fibres. For ductile fibres, on the other hand, plastic bending may accommodate the extra strain at the convex portion of the fibre during withdrawal from the matrix, and may contribute significantly to the total work of fracture. If fibres make a small enough angle to the fracture plane, they will be unable to pull-out, at least initially, and will either fail in shear, or will break through the matrix. Fragmentation of the matrix during failure by such a mechanism further increases the work required, although this contributes only a very small increase relative to the other mechanisms. The fracture surface of a glass–ceramic/discontinuous nickel filament composite is shown in Fig. 13, illustrating the mechanisms of fibre pull-out, plastic bending and rupture of fibres, and matrix fragmentation [145].

The thermal expansion difference between fibre and matrix is a very important parameter in any composite system, since it determines the residual stress–strain

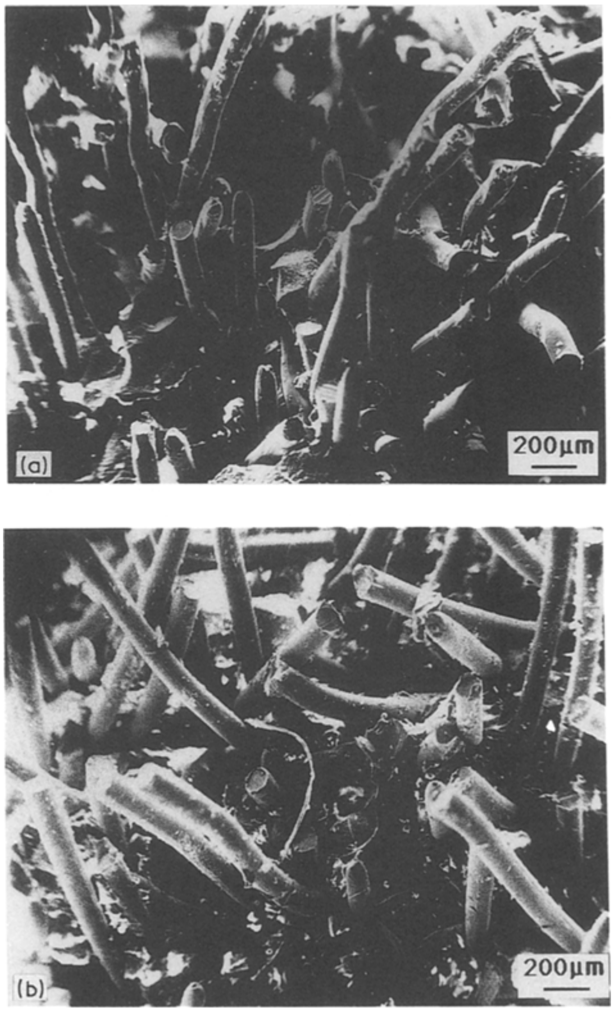

Figure 13 Fracture surfaces of a glass–ceramic composite containing 40 vol % discontinuous nickel filaments 125 µm diameter showing the effects of fibre pull-out, fibre deformation–plastic failure, and matrix fragmentation; after [145].

distributions after fabrication, and can significantly influence the resultant mechanical properties. The residual thermal strain, ε'_m, experienced by the matrix when unidirectionally aligned fibres of different thermal expansions are employed may be assessed semi-quantitatively, assuming interfacial decohesion does not occur in the case of negative $\Delta\alpha$, using the following relationship

$$\varepsilon'_m = E_f V_f \Delta\alpha \, \Delta T / E_c \tag{12}$$

where E_f is Young's modulus of the fibre, ΔT the difference between the fabrication temperature and the ambient temperature, and E_c Young's modulus of the composite.

If the value of ε'_m is positive, the matrix will be in a state of tension; this will give rise to a microcracked system if $\varepsilon'_m > \varepsilon_m$, where ε_m is the normal failure strain of the unreinforced matrix. Conversely, if ε'_m is negative, the matrix will be in compression.

For a given system, the failure stress of the composite, σ_c, may be given by

$$\sigma_c = E_c(\varepsilon_m - \varepsilon'_m) \tag{13}$$

Assuming that the simple rule of mixtures criterion is obeyed

$$E_c = E_m V_m + E_f V_f \tag{14}$$

The corresponding strain experienced by the fibres is given by

$$\varepsilon'_f = -E_m V_m \Delta\alpha \Delta T / E_c \tag{15}$$

The optimum strength for a given system corresponds to the situation where the failure stress of the fibre is reached simultaneously with the failure strain of the matrix. More detailed fibre reinforcement theories and concepts, applied to general composite materials, can be found elsewhere, e.g. Hale and Kelly [146].

A summary of the contrasting factors contributing to the strength and toughness of glass and glass–ceramic matrix composites is given in Table VIII.

Reinforcement of ceramic materials by fibres produced some very encouraging results in the 1960s and 1970s in terms of providing composites with high values for work of fracture. Materials included, for example, a lithium zinc silicate glass–ceramic reinforced by nickel with a work of fracture approaching $17\,\text{kJ}\,\text{m}^{-2}$ [145]; a cordierite glass–ceramic containing SiC filaments with a work of fracture of around $20\,\text{kJ}\,\text{m}^{-2}$ [143]; and a number of carbon fibre reinforced glass and glass–ceramic composites exhibiting works of fracture of up to around $10\,\text{kJ}\,\text{m}^{-2}$ [147–151]. Much of this early work, up until around the mid 1970s, has been reviewed in detail by Donald and McMillan [152].

TABLE VIII Factors promoting strength and toughness in glass and glass–ceramic matrix composites

(a) *FOR HIGH STRENGTH*

1. Modulus of fibre > modulus of matrix
2. Continuous, aligned fibres for maximum strength in one direction
3. Use small diameter fibres (e.g. $\theta < 25\,\mu\text{m}$)
4. Controlled bonding between fibre and matrix

(b) *FOR HIGH TOUGHNESS*

1. Allow local microcracking of the matrix to reduce stress-concentration effects, e.g. by providing weak fibre–matrix bonding
2. Allow extensive fibre pull-out
3. Use ductile fibres

In general, early work concerned with the reinforcement of ceramics by metal or ceramic filaments, although providing substantial improvements in fracture toughness, particularly when using metal reinforcement, unfortunately led to little improvement, or even a reduction, in the mechanical strength [152]. This was because the relatively large diameter fibres employed, normally greater than $50\,\mu\text{m}$ and often as large as $200\,\mu\text{m}$, acted as stress concentration sites which weakened the matrix; toughness was therefore increased at the expense of strength. Notable exceptions where improvements in strength were achieved included some glasses reinforced by tungsten filaments [153, 154]. Simultaneous increases in toughness and strength were also observed by Phillips and co-workers [147–151], for unidirectionally aligned carbon fibre reinforced glasses and glass–ceramics, and by Levitt [155] for carbon fibre reinforced lithium alumino-silicate ceramics containing a glassy phase. Carbon fibres were the only high quality, small diameter ($\approx 8\,\mu\text{m}$) fibres available at that time. Maximum strengths up to around 900 MPa were achieved for these systems, with works of fracture approaching $10\,\text{kJ}\,\text{m}^{-2}$. Significant strengthening was possible due to a combination of factors, including the influence of small fibre size and the large difference in elastic modulus between the carbon fibres and the relatively low modulus glasses and glass–ceramics (relative to many other ceramic materials; for example, alumina and silicon nitride). For systems of this type, where high modulus, small diameter fibres are incorporated into a low modulus matrix, Aveston *et al.* [156] have shown that the cracking strain of the matrix, ε_m, (and hence fracture strength) can be increased, according to the relationship

$$\varepsilon_m = (12\tau\gamma_m E_f V_f^2 / E_c E_m^2 r V_m)^{1/3} \tag{16}$$

where τ is the frictional bond strength, γ_m the work of fracture of the matrix, and r the fibre radius.

Although the carbon fibre composites were quite impressive with respect to high strength and toughness at ambient temperatures, they were not suitable for use at elevated temperatures above 400 °C in oxidizing environments. This was because carbon is readily oxidized, and protection by the matrix is limited due to the phenomenon of matrix microcracking that occurs under stress, this allowing ingress of oxygen to the fibres.

Another notable exception, where high toughness coupled with high strength was achieved, was for a cordierite glass–ceramic reinforced by relatively large diameter ($\approx 100\,\mu\text{m}$) SiC fibres [143]. This system was unique in that the strengthening effect was attributable to the influence of the higher thermal expansion fibres, which were strongly bonded to the matrix, placing the matrix in compression on cooling from the fabrication temperature. As the high strength relied on a thermal expansion difference, however, the strength decreased with increasing temperature. In addition, the fibre was expensive, being produced by chemical vapour deposition of SiC onto a 12 μm diameter tungsten filament substrate.

After the initial great enthusiasm shown in fibre reinforced ceramic composites in the 1960s and early 1970s, interest declined sharply by the mid-to-late 1970s, because of the difficulties outlined above, which were coupled with the general lack of suitable inexpensive small diameter, high strength and high modulus fibres capable of promoting simultaneous increases in both strength and toughness.

Over the last few years, however, a remarkable revival in interest has taken place in the field of ceramic matrix composites due to the advent of a whole new generation of high-performance, small diameter fibres, available commercially at realistic prices. There is now available, for example, a diverse range of ceramic fibres with diameters down to a few micrometres, including silicon carbide and alumina, in addition to coated carbon fibres with improved oxidation resistance. A selection of commercially available fibres is summarized in Table IX.

Reinforcement of glasses and glass–ceramics still offers the best scope for accomplishing simultaneous increases in both strength and toughness, because of the relatively low elastic modulus of these materials. For example, lithium alumino–silicate glasses and glass–ceramics reinforced by silicon carbide fibres with strengths in the range ≈ 600 to 1550 MPa and fracture toughnesses up to $K_{Ic} \approx 27.5$ MPa m$^{1/2}$ have been reported [157–160]. The value of strength of 1550 MPa coupled with a fracture toughness of 27.5 MPa m$^{1/2}$ is, in particular, an astonishing achievement for a ceramic based material [157]. Other work on silicate glasses and glass–ceramics reinforced with SiC fibres has been reported [161–169]. In particular, recent work by Dawson *et al.* [169] has indicated that pyrex glass reinforced by SiC fibres can yield composites which exhibit strengths up to ≈ 1250 MPa, coupled with values for work of fracture of the order of 50 kJ m^{-2}. Oxynitride glass–ceramics have also been investigated, including a Ba–Si–Al–O–N system

TABLE IX Fibre availability and properties

Fibre	Diameter (μm)	Trade name	Manufacturer	Thermal expansion (10^{-6} C^{-1})	Maximum use Temperature (°C)	Tensile strength (MPa)	Modulus (GPa)
(a) *Ceramic fibres*							
Alumina	20	FP-Alumina	DuPont	8.5	1370	1380	380
Alumina	2–4	RF-Saffil	ICI	8.5	1400	1035	300
Alumino-silicate	2–4	Fibermax	Carborundum	–	1650	–	–
Alumino-borosilicate	10	Nextel 440	3M	–	1425	1725	205–240
Zirconia-silicate	14	Nextel Z11	3M	–	1000	1310	75
Silicon carbide	10–15	Nicalon	Nippon Carbon Co.	3.1	1000	2750	200
Boron nitride	–	–	Carborundum	–	2480 (760 in oxidizing environment)	1990	420
Fused silica	1–40	–	Various	0.5	< 1100	–	70
Carbon	7–8	Various	Various	0 (axial) 8 (radial)	< 400 in oxidizing environment	1500–3000	250–400
Metal-coated carbon	8	Cycom	Cyanamid	–	< 1000	3000	235
Silicon carbide	140	SCS	AVCO	4.9	< 1000	3800	400
Boron	100–140	–	AVCO	4.5	–	3600	400
(b) *Metal filaments*							
Die-drawn metals	> 25	–	Various	$\approx$ 5–20	< 1000	400–4000	< 400
Taylor-wire	1–100	–	Experimental only	$\approx$ 5–20	< 1500	< 4400	< 400
Wollaston metal filament tows (316 stainless steel, Inconel 601, Hastelloy X, Ni, Ti)	4–22	Bekinox	Bekaert	$\approx$ 9–20	< 1000	< 1500	< 220
(c) *Whiskers*							
SiC whisker	0.6 (length, 10–80 μm)	SC-9	ARCO	–	–	6890	689
SiC whisker	0.05–0.2 (length, 10–40 μm)	SCW	Tateho	–	–	2100	480
SiC whisker	0.1–0.5 (length, 50–200 μm)	Tokamax	Tokai Carbon	–	< 1600	< 14000	< 700
SiC whisker	3–11 (length, up to 100 mm)	VLS	LANL	–	–	–	–
Si_3N_4 whisker	–	–	Tateho	–	< 1500	1370	380

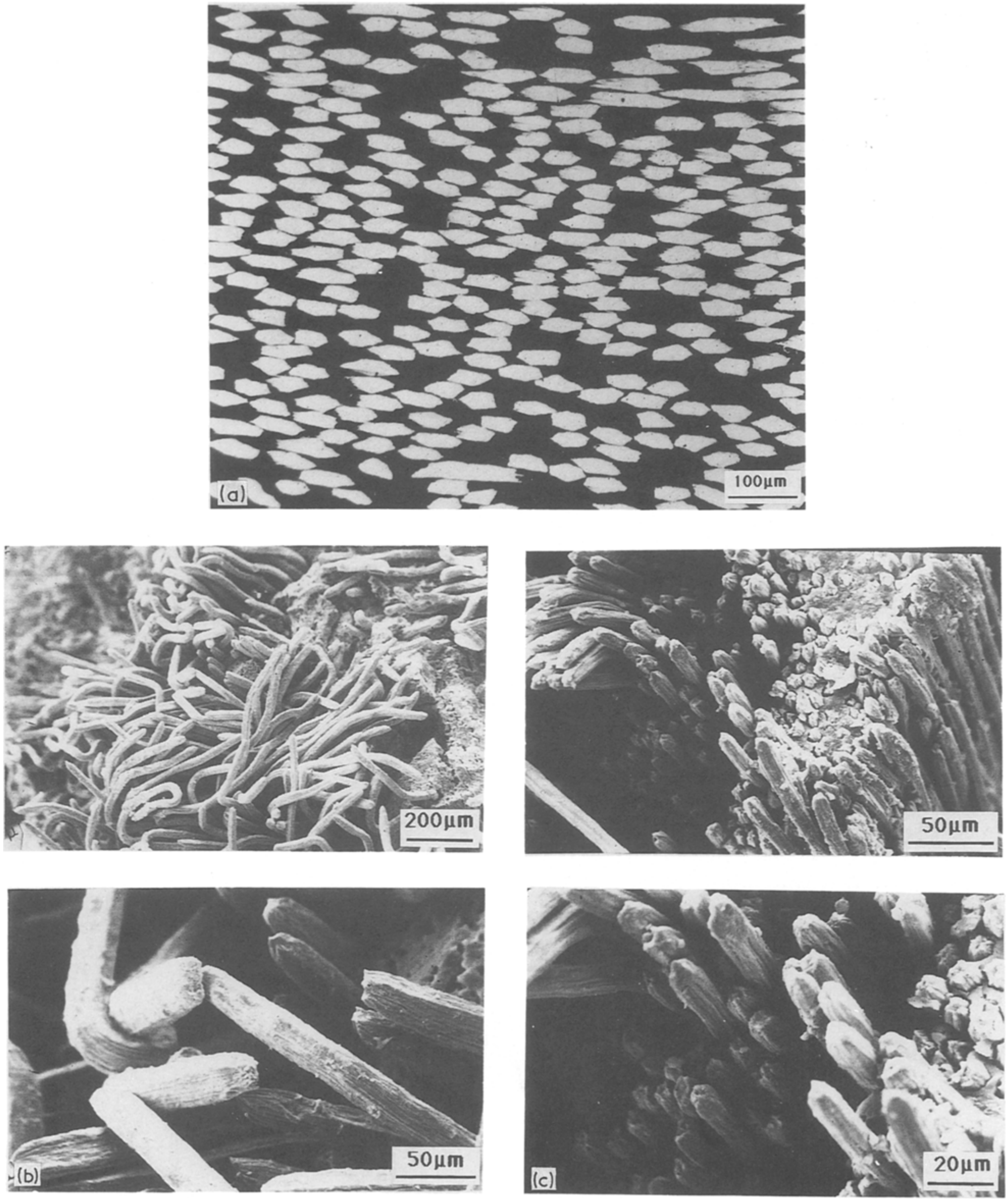

Figure 14 Lithium zinc silicate glass–ceramic/stainless steel filament reinforced composites, after [187]. (a) micrograph of sectioned composite containing 40 vol % continuous, aligned 22 μm diameter filaments; (b) fracture surface of similar 20 vol %, 22 μm composite; (c) fracture surface of similar 20 vol %, 8 μm composite.

reinforced with SiC fibres, with a bending strength of 275 MPa [170]. Various glass–alumina fibre systems have also been examined [171], with strengths in bending to around 300 MPa and fracture toughness values up to 4.0 MPa $m^{1/2}$. It was noted that the highest strengths were obtained for systems of matched thermal expansion. (That optimum strengths are obtained for matched thermal expansion systems has been emphasized previously by Donald and McMillan [152]. They compared the range of strengths reported for various ceramic–matrix systems with the theoretical values, and showed that the best results were generally obtained when $\Delta\alpha$ tends towards zero.) A revival of interest in carbon fibre reinforced glasses and glass–ceramics is also underway [172–177], driven by potential intermediate temperature applications for these materials. A number of reviews are available which report in more detail some of the work up to the early 1980s on this new generation of materials [178–186].

The majority of the recent work has concentrated on using the new ceramic fibres. Metal reinforcement, on the other hand, does offer a number of distinct advantages over ceramic fibres, including a lower susceptibility to damage and degradation during composite fabrication. At the present time, unfortunately, conventional die-drawn metal filaments are either of too large a diameter to promote significant strength increases, due to the reasons outlined earlier, or materials that are available in smaller sizes are prohibitively expensive. Metal filament tows, prepared most probably by the Wollaston route, with individual filament diameters down to around $4\,\mu$m are, on the other hand, available commercially at the present time, and these do offer scope for composite fabrication, although they are only available in a very limited number of materials at the present time. A number of these materials have been used for reinforcing glass–ceramic matrices by Donald and co-workers [187]. Some micrographs are shown in Fig. 14. In addition, a revival of interest is taking place in the production of small diameter metal filaments in a very wide range of metals and alloys directly from the melt, using the Taylor-wire route, as reviewed recently by Donald [188]. In this intrinsically inexpensive process, a fine glass-encapsulated metal filament is produced by the drawing down of a glass tube containing the molten metal or alloy. With suitable control of the process parameters, it is feasible to produce metal filaments with diameters in the range ≈ 1 to $100\,\mu$m, with glass coating thicknesses of around 2 to $30\,\mu$m. The fact that the metal filament is produced directly with a glass coating offers the possibility of preparing glass matrix composites directly from suitable Taylor-wires; and the viability of this route for preparing composites has indeed been shown recently [189]. A typical micrograph of a sectioned glass-matrix composite reinforced by copper filaments of average diameter of about $6\,\mu$m, which has been prepared directly from Taylor-wire, is shown in Fig. 15. In principle, it should be possible to prepare more practical small diameter, high-strength, oxidation resistant filaments of the superalloy variety using the Taylor-wire route, although little work has been reported in this area. It should also be feasible to employ a glass–ceramic precursor coating, from which a more practical and more refractory glass–ceramic composite could be prepared directly, by suitable choice of heat-treatment schedule after consolidating the glass matrix. It is possible that very useful composites could be prepared using such materials.

The requirements of a relatively strong bond between fibre and matrix to promote strength and, for brittle fibre systems, a weak interface to promote toughness, can be reconciled to some degree in duplex fibre systems [190–192]. In these materials, a duplex fibre element is employed consisting of an outer sheath which is bonded strongly to the matrix, and an inner core element which is less strongly, e.g. frictionally, bonded. If failure of the sheath occurs, pull-out effects are still observed between the sheath and inner core element.

The failure behaviour of a ceramic composite is interesting. At low volume fractions of fibre, the failure mode is very similar to that obtained for a monolithic homogeneous ceramic. At higher concentrations, however, a load–displacement curve is obtained which, in many respects, models that of a ductile metal, as illustrated in Fig. 16. A linear region is noted initially at low loads, but at some point deviation from linearity occurs due to the onset of significant matrix microcracking. Above this "proportional limit" a non-linear regime is then encountered as progressive and multiple microcracking of the matrix continues, and fibres undergo the effects of pull-out and/or deformation. Finally, on further deformation, the load decreases, although total strains of several % may be achieved before the load finally approaches the zero level.

Specific data for mechanical strength and toughness

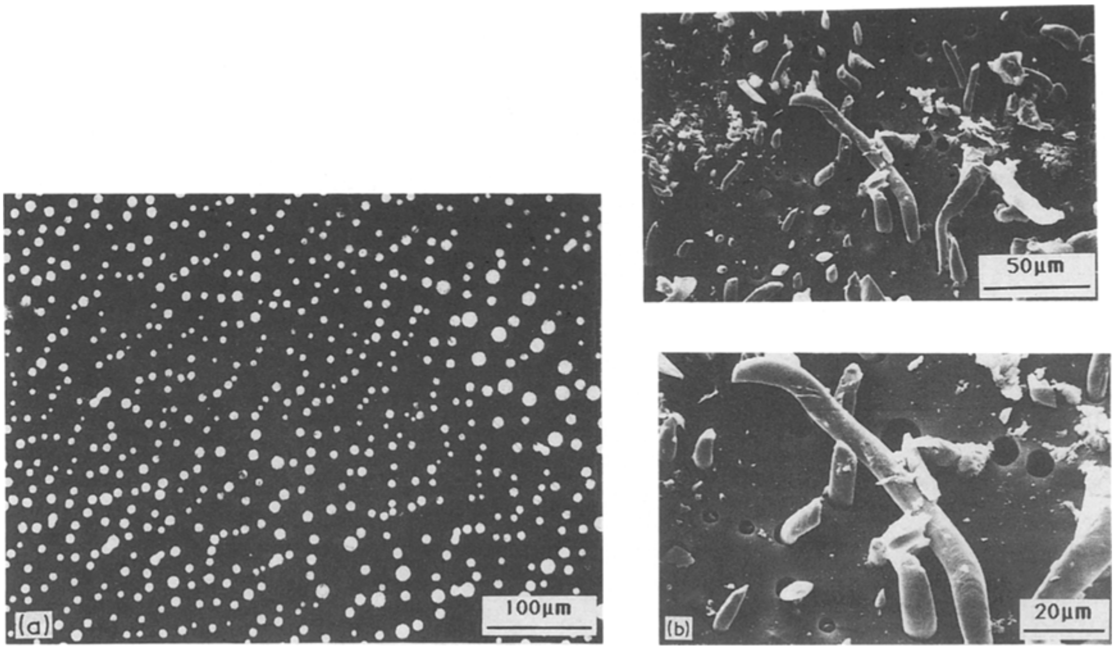

Figure 15 Glass–matrix composite prepared from Taylor-wire; after [189]. (a) micrograph of sectioned sample, (b) fracture surface of composite.

for a variety of fibre reinforced glass and glass–ceramic matrix systems are summarized in Table X and Figs 17 and 18.

3.2.4. Whisker reinforcement

Whiskers are small, single crystal filaments, normally about 0.1 to 10 μm in diameter with aspect ratios of the order of 10 to 100, although higher aspect ratios have been achieved, with some reports of whiskers up to 100 mm in length (see e.g. [193]). In their as-produced state, whiskers can exhibit extremely high strengths, with values approaching the theoretical limit. Their properties are, however, very susceptible to mechanical damage and therefore, in practice, maximum useful strengths are generally limited to less than 1500 MPa.

A summary of work on ceramic–matrix composites reinforced by ceramic whiskers has been given by Bracke *et al.* [194]. More recent work involving SiC whiskers includes that of Wei and Becher [195] using a range of ceramic matrices, Chokshi and Porter [196] using an alumina matrix, and Claussen *et al.* [197] and Becher and Tiegs [198] using zirconia. There has been little reported work specifically on whisker reinforcement of oxide glasses and glass–ceramics, although Gadkaree and Chyung [199] have reported some work in this area. Glasses studied in their investigation included an alumino–silicate composition, together with soda–lime–silica and borosilicate glasses. Barium-stuffed cordierite and barium–osumilite glass–ceramics were also used. The resultant composite strength was found to be dependent on a number of factors, including whisker–matrix thermal expansion mismatch and matrix chemical composition. It was noted that poor composite performance was obtained for either a positive or negative expansion mismatch. Work on glass and glass–ceramic materials reinforced by SiC whiskers has also been reported by Layden and Prewo [200]. Data are summarized in Table X.

3.2.5. Directionally solidified or crystallized structures

A number of fibre reinforced composite systems have been prepared by unidirectional solidification. Some of the materials that have been produced by this route have been reviewed by Donald and McMillan [152]. Related unidirectional crystallization techniques have also been applied to a limited number of glassy materials in order to produce aligned fibre reinforced glass–ceramic systems. For example, Atkinson and McMillan [201] produced preferred orientation of needle-like lithium disilicate crystals in Li_2O–SiO_2–P_2O_5 glasses by extruding partially crystallized material through a die at 800 to 880 °C. Abe *et al.* [202] have also reported the formation of calcium phosphate glass–ceramics reinforced with β-$Ca(PO_3)_2$ fibres by unidirectional crystallization of a glass employing a temperature gradient furnace.

3.2.6. Combined methods

A combination of particle and fibre or whisker reinforcement has been utilized in a limited number of cases; for example, by Becher and Tiegs [198] for a mullite matrix. The simultaneous use of more than one reinforcing mechanism is applicable in principle to most systems, including glasses and glass–ceramics, although little work has been reported in this area.

3.2.7. Glass laminates

Oxide glasses are employed in a number of important composite transparencies, including automobile and aircraft windshields, and bullet-proof glass [203, 204]. Bullet-resistant glass, for example, consists of alternate layers of a transparent thermoplastic and an oxide glass to form a composite sandwich, and is normally composed of three discrete sections; these include a forward facing impact section, a middle transition region, and a final energy absorbing layer. The first section usually consists of a polyvinyl acetal material, for example polyvinyl butyral, sandwiched between two relatively thick layers of glass. The transition region may consist of a relatively thick polyurethane section, whilst the final energy absorbing layer consists of a sheet of polycarbonate material. The total number and thicknesses of laminations can be varied, depending on the precise application in question. For applications requiring very strong but lightweight structures, thermal or chemically strengthened glasses may be used in the laminate.

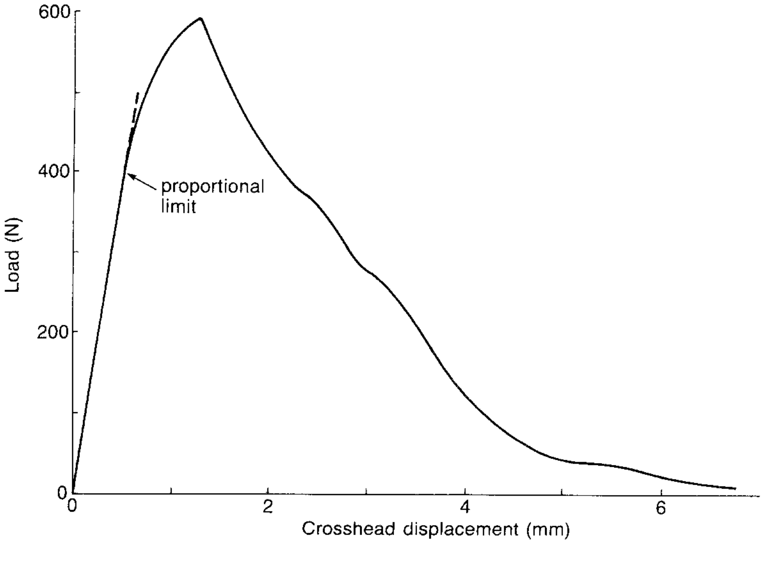

Figure 16 Load–displacement curve illustrating the fracture behaviour of a 40 vol %, 22 μm diameter metal filament reinforced lithium zinc silicate glass–ceramic; after [187].

TABLE X Properties of fibre- and whisker-reinforced glass and glass–ceramic matrix

Matrix	Fibre			Composite flexural strength		Work of fracture ($kJ\,m^{-2}$)	Fracture toughness ($MPa\,m^{1/2}$)	Elastic modulus (GPa)	Reference
	Type	Diameter (μm)	Volume fraction	Absolute (MPa)	Normalized				
(a) *Discontinuous, randomly aligned reinforcement*									
Fused silica	W	50	0.30	275	5.7	–	–	–	[154]
Pyrex glass	W	50	0.15	85	1.2	–	–	–	[153]
LZS glass–ceramic	Ni	125	0.08	130	0.6	5.0	–	–	[145]
			0.40	180	0.8	15.7	–	–	[145]
Pyrex glass	C	7–8	0.20	60	0.6	0.4	–	–	[148]
(b) *Continuous, aligned reinforcement*									
Pyrex glass	C	7–8	0.40	680	≈ 7	3.4	–	–	[147]
LAS glass–ceramic	C	7–8	0.46	575	≈ 3	10.3	–	–	[179]
Pyrex glass	C	7–8	0.43	785	≈ 8	–	–	169	[172]
Cordierite glass–ceramic	SiC	100	0.30	680	≈ 6	20.0	–	–	[143]
LAS glass–ceramic	SiC	10–15	0.50	700	≈ 4	–	17.0	118	[158]
				*830	–	–	25.0	100	[158]
Alumina-silicate glass	SiC	10–15	0.50	1380	≈ 12	–	27.5	–	[157]
MAS glass–ceramic	SiC	10–15	0.40	480	3.5	–	–	–	[159]
LAS glass–ceramic	SiC	10–15	0.40	930	5.4	–	–	124	[159]
Pyrex glass	SiC	10–15	0.49	1250	≈ 12	50	26.3	120	[169]
Pyrex glass	C	7–8	0.55	826	–	–	–	193	[177]
SBS glass + 1% Nb_2O_5	C	7–8	0.42	971	–	–	–	173	[177]
Various glasses	Al_2O_3	–	0.41–0.47	200–311	–	–	2.6–4.0	–	[172]
LZS glass-ceramic stainless	steel	22	0.40	500	≈ 3	50	–	–	[187]
(c) *Whisker reinforcement*									
Corning 1723 glass	SiC	0.6 (10–80 μm long)	0.30 (wt)	338	–	–	3.4	142	[199]
Barium osumilite glass–ceramic	SiC	0.6	0.30 (wt)	400	–	–	4.5	156	[199]
				*300	–	–	7.2	–	[199]
Barium stuffed cordierite glass–ceramic	SiC	0.6	0.3 (wt)	358	–	–	4.5	186	[199]
				*310	–	–	3.5	–	[199]

*Tested in air at 1000° C
LZS—lithium zinc silicate
LAS—lithium alumino-silicate
MAS—magnesium alumino-silicate
SBS—sodium borosilicate

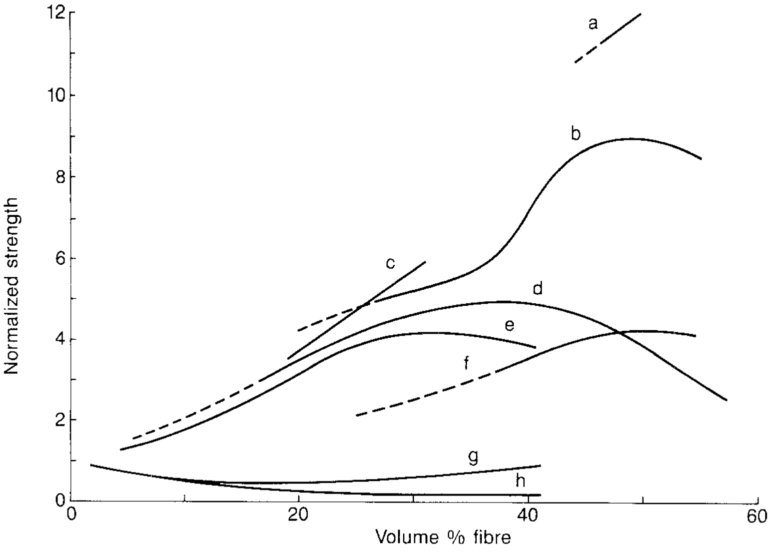

Figure 17 Normalized strength of fibre-reinforced glass and glass-ceramic composites as a function of fibre content. (a lithium alumino-silicate glass–ceramic + silicon carbide fibre; after [157], b pyrex borosilicate glass + carbon fibre; after [177], c silica + tungsten filaments; after [154], d pyrex borosilicate glass + carbon fibre; after [149], e cordierite glass-ceramic + 100 μm diameter silicon carbide fibre; after [143], f pyrex borosilicate glass + carbon fibre; after [147], g lithium zinc silicate glass-ceramic + 125 μm diameter nickel filaments, after [145], h pyrex borosilicate glass + carbon fibre; after [148].)

3.3. Preparation of ceramic composites

Ceramic matrix composites can be prepared by a number of routes. Probably the most widespread is hot-pressing. Randomly orientated fibre and whisker reinforced systems may be prepared by tumbling or high speed blending of fibre–matrix powder mixtures followed by loading into a suitable die and pressing at elevated temperature, usually *in vacuo* or inert atmosphere. Densities approaching 100% of theoretical can readily be achieved by this route, particularly when employing glass or precursor glass–ceramic matrix materials. Graphite dies and punches are often employed; this is due to the ease of machining this material, coupled with its low thermal expansion and chemical inertness, although pressing must be carried out in an inert atmosphere because of its poor oxidation resistance. Dies fabricated from stronger and more abrasion resistant materials, including stainless steel, silicon carbide and TZM (Ti-Zr-Mo) alloy, have been employed, but are less versatile than graphite. During hot pressing, some alignment of the fibres generally occurs so that they tend to lie in the plane of pressing, but within this plane they are randomly orientated. Unidirectionally aligned fibre systems have been prepared by several techniques, including passing continuous fibres through a slurry of matrix powder and binder [205], and extruding fibre–matrix slurries containing ammonium alginate into an acid fixing bath which yields a tape of aligned fibres [206]. In both cases, the tapes can be cut into desired lengths or shapes and hot pressed after a suitable heat treatment to remove the binder. Sol–gel techniques may also be employed to produce particle or fibre reinforced composites (e.g. [140, 207]). Melt-infiltration has been employed with some success (e.g. [208]). Further details covering fabrication of ceramic composites in general are given elsewhere [179, 209, 210].

4. Comparison of methods for improving the mechanical properties of oxide glasses and their limitations

Surface modification of glass, in the form of application of a thin protective coating to pristine or etched glass surfaces, has found widescale use in the glass industry for both bulk materials including containers, and for materials in the form of fibres [76–81]. Any improvement in properties obtained using many of these techniques is, however, easily lost through the

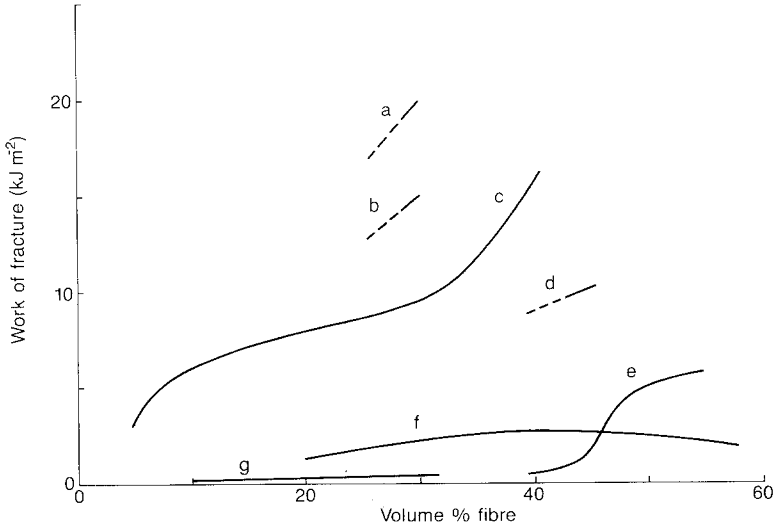

Figure 18 Work of fracture of fibre-reinforced glass and glass–ceramic matrix composites as a function of fibre content. (a cordierite glass–ceramic + 100 μm diameter silicon carbide fibre; after [143], b silica + carbon fibre; after [143], c lithium zinc silicate glass–ceramic + 125 μm diameter nickel filaments; after [145], d lithium alumino-silicate glass-ceramic + carbon fibre; after [179], e and f pyrex borosilicate glass + carbon fibre; after [147, 149], g pyrex borosilicate glass + discontinuous carbon fibre; after [148].)

introduction of relatively minor damage, particularly surface scratches more than a few micrometres in depth – although more recently thicker polymer coatings have been applied to glass surfaces, and these can provide quite significant improvement to accidental damage.

Very large improvements in strength and resistance to quite serious damage can, on the other hand, be imparted through thermal or chemical strengthening treatments that rely on producing a relatively thick compressive layer on the surface of glass articles. Thermal strengthening is, due to the nature of the process, limited to glass articles of relatively simple shape and of thickness greater than 1.5 to 2 mm. In addition, the magnitude of the compressive stress obtainable is restricted by such factors as the thermal expansion characteristics of the glass and the maximum cooling rate achievable in practice. As the glass is quenched from a temperature higher than T_g, viscous deformation and distortion of the glass may also be difficult to avoid completely, an important constraint when designs requiring very close dimensional tolerances are required. Due to the parabolic nature of the stress distribution, once a glass article has been thermally treated to produce a compressive layer of practical magnitude, it cannot be further machined by cutting or drilling, due to the high internal tension. This is in contrast to chemically strengthened glasses where a much flatter stress profile is found and where, depending on the compressive layer thickness in relation to the total thickness of the treated glass article, a high compressive stress can be generated without producing a high internal tension. If the internal tension is low enough it is then quite feasible to machine a treated glass article by cutting and drilling. At the other extreme it is also possible, using chemical treatments, to induce very high internal tensile stresses, particularly in relatively thin samples; and this is the basis for the so-called frangible or command-break glasses that can be fractured predictably and precisely by application of a small amount of local energy just sufficient to trigger the break. Chemically strengthened glasses are unfortunately more expensive than their thermally strengthened equivalents. This is due in part to the high cost involved in maintaining a molten salt bath facility; for example, salts have to be changed at regular intervals due to a build up of contamination products which reduce the efficiency of the process, and very careful and precise temperature control is required. Degradation in the properties of thermally and chemically strengthened glasses occurs at elevated temperatures due to stress relaxation effects. In addition, in the case of chemical strengthening, ionic diffusion also leads to a reduction in strength, particularly at temperatures approaching or exceeding the treatment temperature, although, under prolonged heating, glass degradation may also occur at temperatures significantly less than this, as illustrated in Fig. 5.

Other methods for imparting surface compressive stresses, including cladding with a lower thermal expansion coating and surface crystallization, are generally less versatile than thermal or chemical treatments. In addition, they may also suffer from surface spalling effects due to the very sharp transition obtained between compression and tension; this is particularly severe in the case of surface crystallization.

In the case of glass–ceramic materials, control or tailoring of the thermal expansion characteristics is one of their major attributes. This control can be achieved by careful selection of the precursor glass composition and the heat-treatment schedule. By control of the expansion, it is possible to tailor materials for specific applications, including ceramic-to-metal and ceramic-to-ceramic seal devices, and composite materials. Many other properties, including those of an electrical, chemical or physical nature, can also be tailored according to the initial glass composition and heat-treatment schedule adopted. In addition, conventional, relatively low temperature glass-forming techniques can be employed to produce articles of complex design. Controlled heat treatment may then be carried out in order to provide superior glass–ceramic components possessing higher strength and toughness, higher temperature stability and better abrasion resistance than the equivalent glassy counterpart. A glass–ceramic, although exhibiting higher fracture toughness than the precursor glass still behaves, however, as a highly brittle material, and in particular is prone to catastrophic failure. Only composite systems can provide really significant practical improvements in the fracture toughness of glass and glass–ceramic materials. Increased fracture toughness can be achieved using particle dispersions, in particular zirconia [138–140], but fibre reinforcement offers the most satisfactory means of substantially increasing fracture toughness, and in particular preventing or minimizing the effects of catastrophic failure, especially at elevated temperatures. In the early work on fibre systems it was noted that toughness was generally increased at the expense of ultimate strength, but later work using the new family of fibres has shown that it is now possible to achieve simultaneous improvements both in strength and toughness. In terms of strength enhancement, the highest strengths are found for unidirectionally aligned fibre systems, tested with the fibres parallel to the tensile axis. Fig. 19 shows the effect on strength of fibre orientation for glass matrix carbon fibre systems. It is clear that strength falls off dramatically for only small variations in fibre orientation. As for all fibre reinforced materials, this factor has serious implications in the design of suitable materials for practical applications where the distribution of stresses may vary significantly from an idealistic unidirectional case.

For any composite system, a major area of concern involves compatibility between the matrix and reinforcing phases. This is a particularly severe problem in ceramic-based composites where high fabrication and potential operating temperatures may be involved, and where differences in thermal expansion characteristics between the constituent phases can lead to severe problems of degradation, either during fabrication or in service, particularly when temperature cycling is involved. Glass–ceramic materials offer an

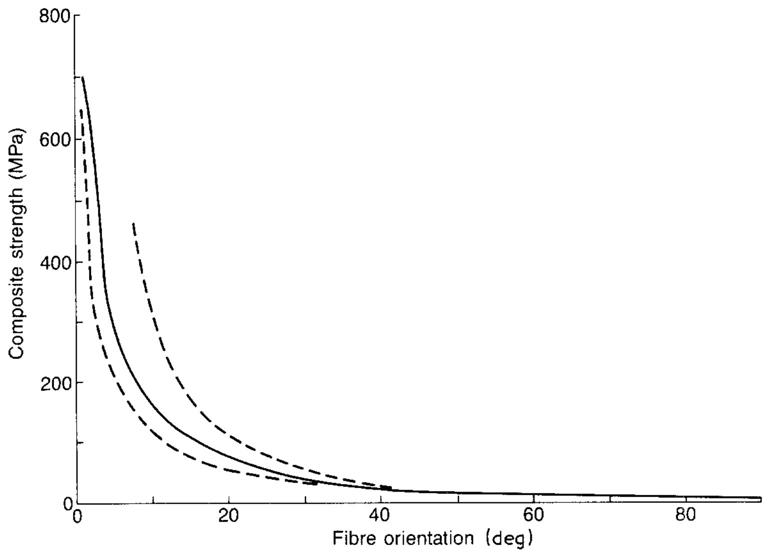

Figure 19 Composite strength as a function of fibre orientation. The broken curve represents range noted for flexural strength of pyrex borosilicate glass–carbon fibre system; after [150]; the full curve is for tensile strength of a similar system; after [172].

important advantage over other matrix materials in this respect because, in principle, the expansion characteristics of the matrix can be tailored to match or at least approximate those of the reinforcing phase. In addition, less severe fabrication conditions, including lower hot-pressing temperatures and pressures, and shorter pressing durations, are in general required to produce fully dense components. This helps to minimize deleterious chemical reactions between the matrix and reinforcement, and leads to less damage of the reinforcing phase during fabrication. A glass–ceramic is particularly advantageous because fully dense composites can be made from the precursor glass at relatively low temperatures. Further heat treatment to crystallize the glass then produces a mechanically stronger and more refractory matrix phase with thermal expansion matched to that of the reinforcement. Some materials, for example carbon fibre reinforced glass and glass–ceramic composites, suffer from the serious disadvantage that they cannot be employed for prolonged periods under stress in an oxidizing atmosphere at temperatures greater than around 400 °C due to degradation of the fibres, as noted in the early work of Phillips and co-workers [147, 205], and re-emphasized recently by Prewo and Batt [176]. These materials are, however, perfectly viable at lower operating temperatures [147, 175], and may fill an important gap between the low temperature polymeric composite systems and the high temperature refractory metal and ceramic systems. In the case of SiC fibre reinforced materials, it has been shown by Chaim and Heuer [163] for a lithium aluminosilicate glass–ceramic matrix, that fibre–matrix reaction, which may lead to a reduction in ultimate strength, can occur during fabrication. This is attributed to the formation of a reaction zone between fibre and matrix which contains amorphous carbon together with NbC microcrystals through which cracks can propagate more readily. Degradation in the strength of similar materials during service at elevated temperatures [160, 166] may be a direct consequence of further matrix–fibre reaction. The search for more thermally stable, high strength composite systems is unfortunately made difficult by the fact that some reaction between fibre and matrix is usually required in order to promote the degree of bonding required for high strength.

The high temperature properties of a selection of glass and glass–ceramic matrix composites are summarized in Fig. 20. In general, these are short duration tests, and holding at a given temperature for prolonged periods of time may lead to degradation of the properties with time.

5. Applications and Future

Many of the materials described in this review have found applications in a widescale and diverse range of subject areas. On the other hand, current applications for some of the materials, in particular the composites, are very limited at the present time, and potential applications must remain highly speculative. A number of applications, both current and potential, are outlined below.

For example, surface modified glasses, particularly thermally strengthened glasses, have found widescale applications as transparencies in the automobile, aircraft and architectural fields. Other applications include spectacle lenses, pressure or vacuum vessel port windows, and containers and pipework in the chemical industry. Chemically strengthened glass, on the other hand, has found far less high production usage, mainly as a result of the higher cost of these materials in relation to their thermally strengthened counterparts. It has been used in automobile, aircraft, helicopter and spacecraft transparencies, spectacle lenses, optical recording discs and as a frangible, command-break material in some military applications, including air-to-ground missile launch tube protective covers. In addition, Beauchamp has proposed [211] that it may be possible to couple a transducer to a frangible glass or glass–ceramic plate, and use the fracture and consequent release of strain energy to trigger an appropriate reaction. A frangible glass–ceramic would be more suitable for applications where a higher energy release is required. (Stephens and Beauchamp have shown experimentally [212] that a chemically strengthened glass disc 25.4 mm in diameter by 3.175 mm thick, yields an energy release

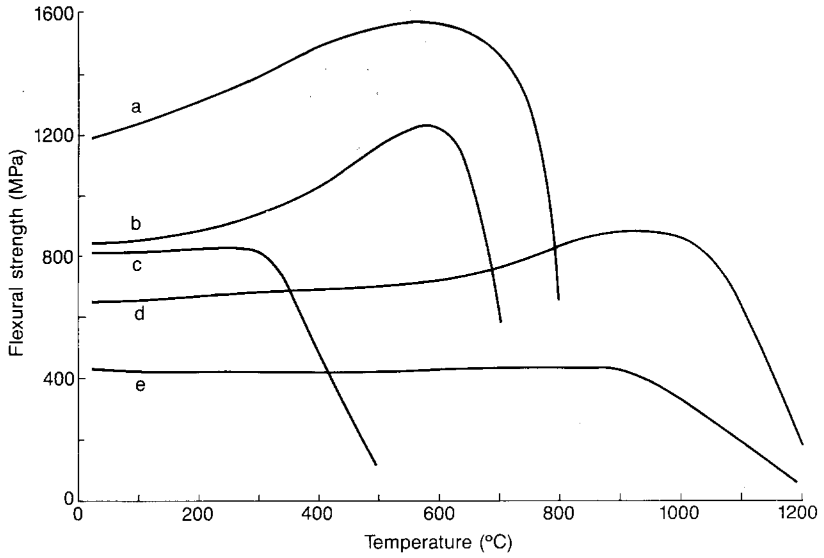

Figure 20 Short duration composite strength as a function of testing temperature in air for a number of systems. (a alumino-silicate glass + 50% silicon carbide fibre; after [157], b pyrex borosilicate glass + 65% silicon carbide fibre; after [180], c lithium alumino-silicate glass–ceramic + 40% carbon fibre (heated in air for 50 h at the temperature indicated and then tested at ambient temperature); after [205], d lithium alumino-silicate glass–ceramic + 50% silicon carbide yarn; after [158], e barium osumilite glass–ceramic + 25% silicon carbide whiskers; after [199].)

of 0.154 J on fracture, whilst a similar glass–ceramic disc delivers a markedly higher value of 1.29 J.) It has also been suggested [213] that, because a change in refractive index of the surface layers of glass is obtained during chemical ion-exchange, such a material could be utilized to prepare tailored light-guiding materials, including graded optical fibres.

Glass–ceramic materials have found applications in such diverse areas as cooking ware and missile radomes. Low thermal expansion glass–ceramics with excellent thermal shock resistance have proved very successful in oven and cooking ware since the introduction of Pyroceram and Corning Ware products by Corning Glass Works nearly thirty years ago. Ceramic cooking hobs have also been constructed from translucent low expansion glass–ceramics, and transparent materials have been used in furnace windows and related areas. Matched thermal expansion glass–ceramic-to-metal seals were first reported by McMillan and co-workers [214–216] in the 1960s. Since then, glass–ceramic materials have been developed with tailored expansion characteristics for sealing to a wide variety of metals, alloys and other ceramics, particularly for electrical and electronics applications [217]. Other uses for glass–ceramic materials include low expansion telescope mirrors, heat exchangers for gas turbines, architectural and nuclear waste disposal materials, microelectronic substrates, and wear resistant bearings and related products [98, 100, 101, 218–226]. Glass–ceramics are also beginning to find important applications in the field of biomedical materials where high strength and hardness combined with chemical inertness and abrasion resistance are important assets [226–229]. In addition, glass–ceramics are now available which can be machined using conventional metal working tools [230, 231]. These materials contain flaky crystals of a fluorophlogopite mica phase ($KMg_3AlSi_3O_{10}F_2$) and can be machined readily due to a combination of easy cleavage of the mica flakes and the crack deflecting properties of the microstructure. They are, therefore, ideally suited for producing complex shapes and are currently used, for example, in the US space shuttle, where over two hundred differently shaped parts are employed, including door hinges and retaining rings.

Glass and glass–ceramic composites, in common with other ceramic-based composite materials, have not yet found widescale applications. This is due in part to the problems and limitations outlined earlier. In addition, ceramic composites have mainly been aimed at providing improvements over existing ceramic and related materials, and providing possible direct replacements for existing technologies. As for all new materials, an alternative approach is to make use of new engineering concepts in which the emerging materials can be tailored to meet the new demands. This, of course, requires close cooperation between materials scientists and design engineers, a union which has not always been totally successful in the past. Potential applications include thermal and ballistic protection shrouds, electromagnetic window materials, turbine and engine components, and biomedical materials. Of these potential application areas, a number show particular promise. For example, carbon and silicon carbide fibre reinforced glass and glass–ceramic composites for biomedical applications, and silicon carbide reinforced cordierite and related glass–ceramic materials for moderately high temperature (≈1000 °C) uses. The area of metal filament reinforced glasses, could also provide a useful extension to organic-based composites, for appli- shows promise for applications requiring high toughness and spalling resistance; for example, ballistic protection and related materials. In addition, glass and glass–ceramic composites, including the carbon fibre reinforced glasses, could also prove a useful extension to organic based composites, for applications in which operating temperatures higher than can currently be met by these materials are likely to be encountered; they could therefore fill a useful intermediate temperature gap in the materials field.

A number of questions remain to be answered, however, before glass and glass–ceramic matrix composites can hope to find more widescale applications and gain greater acceptance as viable engineering materials. In particular, for elevated temperature applications, matrix-reinforcement stability is a major area of concern. More generally, the effect of thermal and mechanical fatigue are also important, and major difficulties remain in the joining or bonding of strengthened components. Due to many of the problems outlined above, in particular matrix-reinforcement compatibility and stability, glass and glass–ceramic composites will be limited to ambient and intermediate temperature applications in the foreseeable future, rather than for prolonged use at elevated temperatures.

The most promising areas will continue to include the reinforcement of materials using the new family of ceramic fibres, particularly as more advanced and more versatile fibres are developed with improved oxidation resistance and a greater resistance to fibre damage during handling and composite fabrication. In addition, for certain applications, use of small diameter metal filaments shows promise and, as outlined earlier, metal reinforcement already offers the major advantage that it is much less readily damaged during composite fabrication. Areas of specific interest include the further development of small diameter Wollaston filaments prepared from more refractory alloys, including the high strength superalloy series, together with the development of more practical Taylor-wire systems; for example, with superalloy cores and precursor glass–ceramic coatings to yield, after consolidation and heat treatment, matched thermal expansion systems. In addition, due to the highly anisotropic properties of unidirectionally aligned fibre systems, which is not a desirable feature for all applications, future studies should include more detailed analyses of multidirectional fibre systems. Such materials have been widely exploited in the polymer composites field, but only to a very limited degree for ceramic–matrix systems. Other potentially promising areas include the simultaneous use of two or more strengthening and toughening techniques. For example, combined use of particle and fibre reinforcement, or use of a surface method in conjunction with a bulk technique; for example, fibre or particle reinforcement combined with chemical strengthening to produce a thin compressive surface layer which is more resistant to the influence of surface defects.

Acknowledgements

The author is indebted to many of his colleagues, including Messrs W. Bradshaw, B. L. Metcalfe and M. J. C. Hill, and Dr C. R. Thomas, for useful discussions. He is also grateful to Mrs. E. A. Prior for carrying out some of the microscopy, and to AWE(A) Technical Services for supplying the figures.

References

1. A. KELLY, "Strong Solids", 2nd edn (Clarendon Press, Oxford, 1973).
2. A. A. GRIFFITH, *Phil. Trans. R. Soc.*, **A221** (1920). 163.
3. *Idem.*, 1st Int. Cong. Appl. Mechanics, Delft (1924) p. 55.
4. C. E. INGLIS, *Trans. Inst. Naval Arch.* **55** (1913) 219.
5. G. KOLOSOFF, *Z. Math. Phys.* **62** (1914) 26.
6. B. E. MOODY, *Glass Technol.* **29** (1988) 73.
7. R. W. DAVIDGE, "Mechanical Behaviour of Ceramics" (Cambridge University Press, Cambridge, 1979).
8. H. G. TATTERSALL and G. TAPPIN, *J. Mater. Sci.* **1** (1966) 296.
9. D. B. MARSHALL and A. G. EVANS, *J. Amer. Ceram. Soc.* **68** (1985) 225.
10. R. ADAMS and P. W. McMILLAN, *J. Mater. Sci.* **12** (1977) 643.
11. T. A. MICHALSKE and S. W. FREIMAN, *J. Amer. Ceram. Soc.* **66** (1983) 284.
12. C. SYMMERS, J. B. WARD and B. SUGARMAN, *Phys. Chem. Glasses* **3** (1962) 76.
13. W. BREARLEY and D. G. HOLLOWAY, *ibid.* **4** (1963) 69.
14. C. K. SAHA and A. R. COOPER, *J. Amer. Ceram. Soc.* **67** (1984) C158.
15. B. R. PROCTOR, *Appl. Mater. Res.* **3** (1964) 28.
16. R. E. MOULD, *J. Amer. Ceram. Soc.* **43** (1960) 160.
17. N. H. RAY and M. H. STACEY, *J. Mater. Sci.* **4** (1969) 73.
18. K. HIRAO and M. TOMOZAWA, *J. Amer. Ceram. Soc.* **70** (1987) 43.
19. B. SUGARMAN, *J. Mater. Sci.* **2** (1967) 275.
20. P. WARD and G. M. BALLARD, US Patent 4205 976 (1980).
21. R. GARDON, in "Glass Science and Technology", Vol. 5, edited by D. R. Uhlmann and N. J. Kreidl (Academic Press, New York, 1980) pp 145–216.
22. S. D. STOOKEY, J. S. OLCOTT, H. M. GARFINKEL and D. L. ROTHERMEL, in "Advances in Glass Technology", VI International Conference, (Plenum, New York, 1962) pp. 397–411.
23. R. W. PETTICREW, L. E. SCHOTT and W. E. SMITH, US Patent 3490 984 (1970).
24. W. KEIFER, W. SACK and D. KRAUSE, US Patent 3907 577 (1975).
25. P. W. McMILLAN, B. P. HODGSON and R. E. BOOTH, *J. Mater. Sci.* **4** (1969) 1029.
26. P. W. McMILLAN, G. PARTRIDGE and J. G. DARRANT, *Phys. Chem. Glasses* **10** (1969) 153.
27. P. W. McMILLAN and G. PARTRIDGE, UK Patent 1108 473 (1968).
28. *Idem.*, UK Patent 1322 796 (1973).
29. G. PARTRIDGE and P. W. McMILLAN, *Glass Technol.* **15** (1974) 127.
30. R. ADAMS and P. W. McMILLAN, *J. Mater. Sci.* **17** (1982) 2727.
31. G. PARTRIDGE, *Glass Technol.* **28** (1987) 9.
32. S. S. KISTLER, *J. Amer. Ceram. Soc.* **45** (1962) 59.
33. R. F. BARTHOLOMEW and H. M. GARFINKEL, in "Glass Science and Technology", Vol. 5, edited by D. R. Uhlmann and N. J. Kreidl (Academic Press, New York, 1980) pp. 217–270.
34. M. E. NORDBERG, E. L. MOCHEL, H. M. GARFINKEL and J. S. OLCOTT, *J. Amer. Ceram. Soc.* **47** (1964) 215.
35. Corning Glass Works, UK Patent 966 732 (1964).
36. *Idem.*, UK Patent 966 731 (1964).
37. F. J. MARUSAK, US Patent 3301 649 (1967).
38. PPG Co. UK Patent 1071 351 (1967).
39. A. L. ZIJLSTRA and A. J. BURGRAAF, *J. Non-Cryst. Solids* **1** (1968) 49.
40. *Idem.*, *ibid.* **1** (1969) 163.
41. A. E. SAUNDERS and R. E. KUBICHAN, US Patent 3433 611 (1969).
42. H. M. GARFINKEL and C. B. KING, *J. Amer. Ceram. Soc.* **53** (1970) 686.
43. K. KOBAYASHI and K. SATO, *Glass Technol.* **19** (1978) 66.
44. I. W. DONALD and M. J. C. HILL, *J. Mater. Sci.*, **23** (1988) 2797.
45. M. J. C. HILL and I. W. DONALD, *Glass Technol.*, **30** (1989) 123.
46. J. CORNELISSEN and A. J. BURGRAAF, in Proceedings 7th International Conference on Glass (Gordon and Breach, New York, 1965) pp 319.1–319.4.
47. J. B. WARD, B. SUGARMAN and C. SYMMERS, *Glass Technol.* **6** (1965) 90.
48. H. GARFINKEL, *Glass Ind.* **50** (1969) 28.

49. C. W. DOYLE and F. J. MARUSAK, US Patent 3524 737 (1970).
50. A. K. VARSHNEYA and R. J. PETTI, *J. Amer. Ceram. Soc.* **59** (1976) 42.
51. D. W. RINEHART, US Patent 4055 703 (1977).
52. M. J. KERPER and T. G. SCUDERI, *J. Amer. Ceram. Soc.* **49** (1966) 613.
53. J. S. STROUD, *Glass Technol.* **29** (1988) 108.
54. V. V. MOISEEV, T. V. PERMYAKOVA and M. N. PLOTNIKOVA, *ibid.* **11** (1970) 6.
55. Glaverbel, UK Patent 1217 660 (1970).
56. T. YOKO, K. KAMIYA, Y. ISHINO and S. SAAKA, *J. Amer. Ceram. Soc.* **69** (1984) C154.
57. J. C. CAPP and J. E. SHELBY, *ibid.* **69** (1986) C110.
58. S. D. STOOKEY, "High Strength Materials", edited by V. F. Zackay (Wiley, London, 1965) pp. 669–681.
59. N. WEBER, US Patent 3218 220 (1965).
60. S. SURNES, *J. Amer. Ceram. Soc.* **56** (1973) 514.
61. H. OHTA, *J. Non-Cryst. Solids* **24** (1977) 61.
62. M. ABOU-EL-LEIL and A. R. COOPER, *Glass Technol.* **21** (1980) 57.
63. *Idem.*, *J. Amer. Ceram. Soc.* **64** (1981) 141.
64. C. K. SAHA and A. R. COOPER, *ibid* **67** (1984) C160.
65. Anon, *Bull. Amer. Ceram. Soc.* **54** (1975) 19.
66. Corning Glass Works, UK Patent 786 951 (1957).
67. Philips Electronic and Associated Industries, UK Patent, 1215 729, 1970.
68. D. A. DUKE, J. F. MacDOWELL and B. R. KARSTETTER, *J. Amer. Ceram. Soc.* **50** (1967) 67.
69. G. H. BEALL, B. R. KARSTETTER and H. L. RITTLER, *ibid,* **50** (1967) 181.
70. Corning Glass Works, UK Patent 1219 193 (1971).
71. A. R. COOPER and D. A. KROHN, *J. Amer. Ceram. Soc.* **52** (1969) 665.
72. O. RICHMOND, W. C. LESLIE and H. A. WREIDT, *Trans. ASM* **57** (1964) 294.
73. P. F. JAMES, paper presented at Symposium on Glass Strength, Society Glass Technology, Harrogate, May 1988.
74. D. A. KROHN and A. R. COOPER, *J. Amer. Ceram. Soc.* **52** (1969) 661.
75. D. A. KROHN, *ibid.* **53** (1970) 505.
76. A. J. DEYRUP, US Patent 2831 780 (1958).
77. P. EHRBURGER, A. MUSIELAK and J. LAHAYE, *Bull. Amer. Ceram. Soc.* **59** (1980) 844.
78. D. K. NATH, *ibid.* **65** (1986) 752.
79. C. M. CARLESS, *Glass Technol.* **28** (1987) 175.
80. K. L. LOEWENSTEIN, "The Manufacturing Technology of Continuous Glass Fibres, Glass Science and Technology", Vol. 6, 2nd edn (Elsevier, Amsterdam, 1983).
81. A. KUSKE and G. ROBERTSON, "Photoelastic stress analysis", (Wiley, London, 1974).
82. R. WELLER, *J. Appl. Phys.* **10** (1939) 266.
83. E. K. BEAUCHAMP and R. H. ALTHERR, *J. Amer. Ceram. Soc.* **54** (1971) 103.
84. W. BRADSHAW, *J. Mater. Sci.* **14** (1979) 2981.
85. A. Y. SANE and A. R. COOPER, *J. Amer. Ceram. Soc.* **61** (1978) 359.
86. *Idem.*, *ibid.* **70** (1987) 86.
87. J. M. BARSOM, *ibid.* **51** (1968) 75.
88. B. R. LAWN and D. B. MARSHALL, *Phys. Chem. Glasses,* **18** (1977) 7.
89. M. BAKIOGLU, F. ERDOGAN and D. P. H. HASSELMAN, *J. Mater. Sci.* **11** (1976) 1826.
90. C. C. HSIAO, "Fracture 1977", Vol. 3, ICF4, Waterloo, Canada, (1977) pp. 985–989.
91. J. CHANG and J. CHOU, *J. Non-Cryst. Solids* **52** (1982) 395.
92. M. M. ABOU-EL-LEIL, F. A. CAMARATTA and R. R. DIGENOVA, *J. Amer. Ceram. Soc.* **68** (1985) C18.
93. M. M. CHAUDHARI and L. LIANGYI, *Nature* **320** (1986) 713.
94. M. M. ABOU-EL-LEIL, F. A. CAMARATTA and R. R. DIGENOVA, *J. Amer. Ceram. Soc.* **69** (1986) 713.
95. D. R. OAKLEY and M. F. GREEN, paper presented at Symposium on Glass Strength, Society Glass Technology, Harrogate, May 1988.
96. I. W. DONALD and B. L. METCALFE, AWE, unpublished work (1983).
97. M. V. SWAIN, J. T. HAGAN and J. E. FIELD, *J. Mater. Sci.* **12** (1977) 1914.
98. P. W. McMILLAN, "Glass ceramics, 2nd edn (Academic Press, London, 1979).
99. Z. STRNAD, "Glass–Ceramic Materials (Elsevier, Amsterdam, 1986).
100. P. W. McMILLAN and G. PARTRIDGE, *Proc. Brit. Ceram. Soc.* **3** (1965) 241.
101. G. H. BEALL, in "Glass Science and Technology", Vol. 1, "Glass Forming Systems", edited by D. R. Uhlmann and N. J. Kreidl (Academic, New York, 1983) pp. 403–443.
102. J. HLAVAC, "The Technology of Glass and Ceramics," (Elsevier, Amsterdam, 1983) pp. 228–243.
103. A. DE, A. K. MOITRA and P. K. GUPTA, *Trans. Indian Ceram. Soc.* **43** (1984) 105.
104. P. W. McMILLAN, S. V. PHILLIPS and G. PARTRIDGE, *J. Mater. Sci.* **1** (1966) 269.
105. M. P. BOROM, A. M. TURKALO and R. H. DOREMUS, *J. Amer. Ceram. Soc.* **58** (1975) 385.
106. D. R. BRIDGE, D. HOLLAND and P. W. McMILLAN, *Glass Technol.* **26** (1985) 286.
107. I. W. DONALD, B. L. METCALFE, D. J. WOOD and J. R. COPLEY, *J. Mater. Sci.* in press.
108. I. W. DONALD and R. A. McCURRIE, *J. Amer. Ceram. Soc.* **55** (1972) 289.
109. Z-X. CHEN and P. W. McMILLAN, *J. Mater. Sci.* **20** (1985) 3428.
110. A. J. STRYJAK and P. W. McMILLAN, *ibid.* **13** (1978) 1794.
111. R. W. RICE, *ibid.* **14** (1979) 2768.
112. M. A. STETT and R. M. FULRATH, *J. Amer. Ceram. Soc.* **53** (1970) 5.
113. C. O. McHUGH, T. J. WHALEN and M. HUMENIK, *ibid.* **49** (1966) 486.
114. R. M. McMEEKING and A. G. EVANS, *ibid.* **65** (1982) 242.
115. V. V. KRSTIC, P. S. NICHOLSON and R. G. HOAGLAND, *ibid.* **64** (1981) 499.
116. T. B. TROCZYNSKI, P. S. NICHOLSON and C. E. RUCKER, *ibid.* **71** (1988) C276.
117. D. P. H. HASSELMAN and R. M. FULRATH, *ibid.* **49** (1966) 68.
118. Y. NIVAS and R. M. FULRATH, *ibid.* **53** (1970) 188.
119. R. R. TUMMALA and A. L. FREIEDBERG, *ibid.* **52** (1969) 228.
120. R. W. DAVIDGE and T. J. GREEN, *J. Mater. Sci* **3** (1968) 629.
121. R. I. BERTOLOTTI and R. M. FULRATH, *J. Amer. Ceram. Soc.* **50** (1967) 558.
122. F. F. LANGE, *Phil. Mag.* **22** (1970) 983.
123. A. G. EVANS, *ibid.* **26** (1972) 1327.
124. V. D. KRSTIC, *ibid.* **A, 48** (1983) 695.
125. J. SELSING, *J. Amer. Ceram. Soc.* **44** (1961) 419.
126. W. J. FREY and J. D. MACKENZIE, *J. Mater. Sci.* **2** (1967) 124.
127. R. C. ROSSI, *J. Amer. Ceram. Soc.* **52** (1969) 290.
128. N. MIYATA and H. JINNO, *J. Mater. Sci.* **17** (1982) 547.
129. T. L. JESSEN, J. J. MECHOLSKY and R. H. MOORE, *Bull. Amer. Ceram. Soc.* **65** (1986) 377.
130. R. C. GARVIE, R. H. HANNINK and R. T. PASCOE, *Nature* **258** (1975) 703.
131. D. L. PORTER and A. H. HEUER, *J. Amer. Ceram. Soc.* **60** (1977) 543.
132. A. H. HEUER, *ibid.* **70** (1987) 689.
133. N. CLAUSSEN, *Z. Werkstofftech.* **13** (1982) 138.
134. N. CLAUSSEN, in "European Coll. Ceramics in Advanced Energy Technologies" (Petten, The Netherlands, 1982) pp. 51–86.
135. F. F. LANGE, *J. Mater. Sci.* **17** (1982) 225.
136. N. CLAUSSEN, *J. Amer. Ceram. Soc.* **59** (1976) 49.
137. R. STEPHENS, An Introduction to Zirconia, Magnesium Elecktron Ltd., Publication No. 13, (1983).
138. S. FAGHERAZZI, S. ENZO, V. GOTTARDI and G. SCARINCI, *J. Mater. Sci.* **15** (1980) 2693.

139. K. KEEFER and T. MICHALSKE, US Patent 4587 224 (1986).
140. M. NOGAMI and M. TOMOZAWA, *J. Amer. Ceram. Soc.* **69** (1986) 99.
141. H. KRENCHEL, "Fibre Reinforcement", (Akademisk Forlag, Copenhagen, 1964).
142. V. LAWS, *J. Phys. D* **4** (1971) 1737.
143. J. A. AVESTON, in "The Properties of Fibre Composites", Conference Proceedings NPL, 1971 (IPC Science and Technology Press, Guildford, 1972) pp. 63–74.
144. A. H. COTTRELL, *Proc. R. Soc.* **A282** (1974) 1.
145. I. W. DONALD and P. W. McMILLAN, *J. Mater. Sci.* **12** (1977) 290.
146. D. K. HALE and A. KELLY, *Ann. Rev. Mater. Sci.* **2** (1972) 405.
147. R. A. J. SAMBELL, A. BRIGGS, D. C. PHILLIPS and D. H. BOWEN, *J. Mater. Sci.* **7** (1972) 676.
148. R. A. J. SAMBELL, D. H. BOWEN and D. C. PHILLIPS, *ibid.* **7** (1972) 663.
149. D. C. PHILLIPS, *ibid.* **7** (1972) 1175.
150. D. C. PHILLIPS, R. A. J. SAMBELL and D. H. BOWEN, *ibid.* **7** (1972) 1454.
151. D. C. PHILLIPS, *J. Compos. Mater.* **8** (1974) 130.
152. I. W. DONALD and P. W. McMILLAN, *J. Mater. Sci.* **11** (1976) 949.
153. G. EINMAHL, UCRL Technical Report 16844, May 1966.
154. R. H. DUNGAN, J. A. GILBERT and J. C. SMITH, *J. Amer. Ceram. Soc.* **56** (1973) 345.
155. S. R. LEVITT, *J. Mater. Sci.* **8** (1973) 793.
156. J. AVESTON, G. A. COOPER and A. KELLY, in "The Properties of Fibre Composites", NPL Conference Proceedings (IPC Science and Technology Press, Guildford, 1972) pp. 15–24.
157. J. J. BRENNAN and K. W. PREWO, UK Patent Appl. GB 2075 490A, 1981.
158. *Idem.*, *J. Mater. Sci.*, **17** (1982) 2371.
159. T. MAH, M. G. MENDIRATTA, A. P. KATZ, R. RUH and K. S. MAZDIYASNI, *J. Amer. Ceram. Soc.* **68** (1985) C27.
160. *Idem.*, *ibid.* **68** (1985) C248.
161. S. LANKFORD, *Composites* **18** (1987) 145.
162. K. M. PREWO, *J. Mater. Sci.* **22** (1987) 2695.
163. R. CHAIM and A. H. HEUER, *Advanced Ceram. Mater.* **2** (1987) 154.
164. K. M. PREWO and J. J. BRENNAN, *J. Mater. Sci.* **15** (1980) 463.
165. *Idem.*, *ibid.* **17** (1982) 1201.
166. E. Y. LUH and A. G. EVANS, *Ceram. Engng Sci. Proc.* **6** (1985) 608.
167. M. P. BOROM and C. A. JOHNSON, *J. Amer. Ceram. Soc.* **70** (1987) 1.
168. R. F. COOPER and K. CHYUNG, *J. Mater. Sci.* **22** (1987) 3148.
169. D. M. DAWSON, R. F. PRESTON and A. PURSER, *Silicates Industriels* **53** (1988) 129.
170. M. A. HERRON and S. H. RISBUD, *Bull. Amer. Ceram. Soc.* **65** (1986) 342.
171. T. A. MICHALSKE and J. R. HELLMAN, *J. Amer. Ceram. Soc.* **71** (1988) 725.
172. V. C. NARDONE and K. M. PREWO, *ibid.* **23** (1988) 168.
173. K. CHYUNG, *J. Mater. Sci.* **22** (1987) 701.
174. L. F. JOHNSON, D. P. H. HASSELMAN and E. MINFORD, *ibid.* **22** (1987) 3111.
175. R. A. ALLAIRE, V. F. JANAS, S. STUCHLY and M. P. TAYLOR, *SAMPE Quarterly* **19** (1987) 25.
176. K. W. PREWO and J. A. BATT, *J. Mater. Sci.* **23** (1988) 523.
177. K. M. PREWO, *ibid.* **23** (1988) 2745.
178. R. W. RICE, in Proceedings 5th Annual Conference Composites and Advanced Ceramic Materials, (Amer. Ceram. Soc., Columbus, Ohio, 1981) pp. 661–701.
179. D. C. PHILLIPS, in "Handbook of Composites", Vol. 4, edited by A. Kelly and S. T. Mileiko (Elsevier, Amsterdam, 1983) pp. 373–428.
180. K. M. PREWO, J. J. BRENNAN and G. K. LAYDEN, *Bull. Amer. Ceram. Soc.* **65** (1986) 305.
181. L. J. SCHIOLER and J. J. STIGLICH, *ibid.* **65** (1986) 289.
182. J. J. MECHOLSKY, *ibid.* **65** (1986) 315.
183. R. W. DAVIDGE, *Composites* **18** (1987) 92.
184. T-I. MAH, M. G. MENDIRATTA, A. P. KATZ and K. S. MAZDIYASNI, *Bull. Amer. Ceram. Soc.* **66** (1987) 304.
185. D. B. MARSHALL and J. E. RITTER, *ibid.* **66** (1987) 309.
186. G. FISHER, *ibid.* **63** (1984) 360.
187. I. W. DONALD, B. L. METCALFE and A. D. BYE, *J. Mater. Sci.* to be submitted.
188. I. W. DONALD, *ibid.* **22** (1987) 2661.
189. I. W. DONALD, B. L. METCALFE and A. D. BYE, *J. Mater. Sci. Lett.* **7** (1988) 964.
190. A. G. EVANS, *J. Mater. Sci.* **9** (1974) 1145.
191. M. J. CHAPPEL and R. S. MILLMAN, *ibid.* **12** (1974) 1933.
192. I. R. McCOLL and J. G. MORLEY, *ibid.* **12** (1977) 1165.
193. E. A. FEEST, *Mater. Design* **7** (1986) 58.
194. P. BRACKE, H. SCHURMANS and J. VORHOEST, in "Inorganic Fibres and Composite Materials", European Patent Office (Pergamon Press, Oxford, 1984) pp. 97–121.
195. G. C. WEI and P. F. BECHER, *Bull. Amer. Ceram. Soc.* **64** (1985) 298.
196. A. H. CHOKSHI and J. R. PORTER, *J. Amer. Ceram. Soc.* **68** (1985) C144.
197. N. CLAUSSEN, K-L. WEISSKOPF and M. RÜHE, *ibid.* **69** (1986) 288.
198. P. F. BECHER, T. N. TIEGS, *ibid.* **70** (1987) 651.
199. K. P. GADKAREE and K. CHYUNG, *Bull. Amer. Ceram. Soc.* **65** (1986) 370.
200. G. K. LAYDEN and K. M. PREWO, UTRC Final Report R85-916943-1 (1985).
201. D. I. H. ATKINSON and P. W. McMILLAN, *J. Mater. Sci.* **10** (1975) 2012.
202. Y. ABE, M. HOSOE, T. KASUGA, H. ISHIKAWA, N. SHIUKAI, Y. SUZUKI and J. NAKAYAMA, *J. Amer. Ceram. Soc.* **65** (1982) C189.
203. G. F. FREEGUARD and D. MARSHALL, *Composites* **11** (1980) 25.
204. R. D. KING and R. W. WRIGHT, *Glass Technol.* **28** (1987) 73.
205. R. A. J. SAMBELL, D. C. PHILLIPS and D. H. BOWEN, in "Carbon Fibres, Their Place in Modern Technology: Proceeding 2nd International Conference Carbon Fibres" (Plastics Institute, London, 1974).
206. C. A. CALOW and R. J. WAKELIN, *J. Inst. Metals* **96** (1968) 147.
207. S. DATTA, S. S. MITRA, D. CHAKRAVORTY, S. RAM and D. BAHADUR, *J. Mater. Sci. Lett.* **5** (1986) 89.
208. W. B. HILLIG, *J. Amer. Ceram. Soc.* **71** (1988) C96.
209. P. BRACKE, H. SCHURMANS and J. VORHOEST, in "Inorganic Fibres and Composite Materials, European Patent Office" (Pergamon Press, Oxford, 1984) pp. 123–135.
210. J. A. CORNIE, Y-M. CHIANG, D. R. UHLMANN, A. MORTENSEN and J. M. COLLINS, *Bull. Amer. Ceram. Soc.* **65** (1986) 293.
211. E. K. BEAUCHAMP, in "Fracture Mechanics of Ceramics", Vol. 2, edited by R. C. Bradt, D. P. H. Hasselman and F. F. Lange (Plenum, New York, 1974) pp. 817–827.
212. H. P. STEPHENS and E. K. BEAUCHAMP, *Bull. Amer. Ceram. Soc.* **53** (1974) 159.
213. W. G. FRENCH and A. D. PEARSON, *ibid.* **49** (1970) 974.
214. P. W. McMILLAN and B. P. HODGSON, *Engineering* **196** (1963) 366.
215. P. W. McMILLAN, B.P.HODGSON and G. PARTRIDGE, *Glass Technol.* **7** (1966) 121.
216. P. W. McMILLAN, G. PARTRIDGE, B. P. HODGSON and H. R. HEAP, *ibid* **7** (1966) 128.
217. G. PARTRIDGE and C. A. ELYARD, *Brit. Ceram. Procs.* **34** (1984) 219.

218. T. R. NASH, E. M. PASHBY and R. L. COLLETT, *Glass Technol.* **24** (1983) 298.
219. G. PARTRIDGE, *ibid.* **24** (1983) 293.
220. M. WADA and S. KAWAMURA, *Bull. Inst. Chem. Res. Kyoto Univ.* **59** (1981) 256.
221. D. G. GROSSMAN, in "Advances in Ceramics 4", edited by J. H. Simmons, D. R. Uhlmann and G. H. Beall (Amer. Ceram. Soc., Columbus, Ohio, 1982) pp. 249–259.
222. G. H. BEALL and D. A. DUKE, in "Glass Science and Technology 1", edited by D. R. Uhlmann and N. J. Kreidl (Academic Press, New York, 1983) pp. 241–257.
223. W. R. PRINDLE, *Ceramica* **29** (1983) 273.
224. I. W. DONALD, AWRE Report No. 0 19/84, HMSO (London), 1984.
225. G. H. BEALL, *J. Non-Cryst. Solids* **73** (1985) 413.
226. W. T. MacCULLOCH, *Brit. Dental. J.* **124** (1968) 361.
227. S. F. HULBERT, L. L. HENCH, D. FORBES and L. S. BOWMAN, in "Advances in Surgery", edited by P. Vincenzini (Elsevier, Amsterdam, 1983) pp. 3–29.
228. G. FISHER, *Bull. Amer. Ceram. Soc.* **62** (1983) 1237.
229. J. W. BORETOS, *Adv. Ceram. Mater.* **2** (1987) 15.
230. G. H. BEALL, in "Advances in Nucleation and Crystallization in Glasses", edited by L. L. Hench and S. W. Freiman (Amer. Ceram. Soc., Columbus, Ohio, 1971) pp. 251–261.
231. D.G.GROSSMAN, *Glass Technol.* **24** (1983) 11.

Received 18 November 1988
and accepted 20 January 1989